

THESIS

**The *MC4R* gene is responsible
for the development of ovarian
teratomas**

December 2020

Shizuoka University
Graduate School of Science and Technology,
Educational Division
Department of Bio-science

(Abdullah An Naser)

Contents

	Page No.
Abstract	3
Abbreviation	4
List of figures	5
Chapter 1 Introduction	6
Chapter 2 Materials and Methods	10
2.1 Mice	10
2.2 Creation of genome-edited mice	11
2.3 Genotyping	12
2.3.1 Genotyping for <i>Ter</i>	12
2.3.2 Genotyping for <i>MC4R</i>	13
2.4 Establishment of gene knock-in or knockout strains	13
2.5 Establishment of double mutant mouse strain	13
2.6 Observation of ovarian teratomas	14
2.7 Histological analysis	14
2.8 Immunohistochemical observation	14
Chapter 3 Results	15
3.1 Creation of genome editing mice	15
3.2 Creation of double mutant mice	16
3.3 Observation of OTs in other mice strains	16
3.4 Search for parthenogenesis from the Knock-in mouse ovary	17
3.5 Immunohistochemistry of Knock-in mouse ovary	17
3.6 Observation of abnormalities in other organs of Knock-in mice	17
Chapter 4 Discussions	19
Chapter 5 References	23
Chapter 6 Figures	29
Appendices	48

ABSTRACT

Teratomas in mice, composed of different tissue types, are derived from primordial germ cells (PGCs) in the foetal gonads. The strongest candidate gene in the teratoma locus (*Ter*) responsible for testicular teratoma formation was identified as *Dnd1*. However, the phenotype of mice with a mutated *Dnd1* gene was germ cell loss. Thus, it was suggested that other genes are involved in teratoma formation. Testicular teratomas can also be induced experimentally (experimentally testicular teratomas: ETTs) in 129/Sv mice by transplanting E12.5 foetal testes into adult testes. Previously, we mapped the *ett1* locus, which is the locus responsible for ETT formation on chromosome 18. We established the LT-*ett1* congenic strain, which introduced the locus responsible for ETT formation genetically into the genomes of a testicular teratoma non-susceptible strain. In this study, we crossed LT-*ett1* and a previously established LT-*Ter* strain to establish the double congenic strain LT-*Ter/ett1*.

Separately, we conducted exome sequence analysis of the 129 and LT strains to identify the genes responsible for ETT formation, and we identified a missense mutation in the *MC4R* gene among 8 genes in the *ett1* region. Thus, this gene is most likely a candidate for ETT formation.

In this study, we tried to establish a strain with a point mutation in the *MC4R* gene of the LT strain by genome editing. After establishing the knock-in strain LT-*MC4R*^{G25S}, we also attempted to establish the double genetically modified strain LT-*Ter/MC4R*^{G25S} to address the relation between *Ter* and *MC4R*.

Surprisingly, highly developed ovarian teratomas (OTs), instead of testicular teratomas, appeared not only in the LT-*Ter/MC4R*^{G25S} and LT-*MC4R*^{G25S} strains but also in the LT-*ett1* and LT-*Ter/ett1* strains. The incidence of OT formation was high in double genetically modified strains. The results demonstrated that *MC4R* is one of the genes responsible for OT formation. It was suggested that the effect of the missense mutation in *MC4R* on teratoma formation was promoted by abnormal germ cell formation by the mutation in *DND1*.

During the study alongside the OTs we also observed other organs as we found some abnormalities in kidney and spleen in LT-*Ter/MC4R*^{G25S} double mutant mice. This study is under investigation to find whether there is any relation with the *MC4R* or not.

The LT-*Ter/MC4R*^{G25S} double-gene-modified line we established was used to reveal the cause of spontaneous testicular teratomas (STT). But, in this study no STT was recorded as the original 129/Sv strain. Morphologically the size of the testis of LT-*Ter*^{-/-}/*MC4R*^{G25S/G25S} is smaller than the LT-*Ter*^{+/-}/*MC4R*^{G25S/G25S} and LT-*Ter*^{+/+}/*MC4R*^{G25S/G25S} individuals as like as other *Ter* congenic and original 129/Sv strains indicating *MC4R*^{G25S} mutant is not responsible for STT formation in males.

Abbreviation

ETT (ett)	experimental testicular teratoma
STT	spontaneous testicular teratoma
SSLP	simple sequence length polymorphism
SNP	single nucleotide polymorphism
129	129/Sv-+/Ter (+/+)
LT	LTXBJ
B6	C57BL/6J
PGC	primordial germ cell
ssODN	single strand oligodeoxynucleotide
MC4R	melanocortin 4 receptor
IGV	integrative genomics viewer
EC	embryonal carcinoma (cell)
ES	embryonic stem (cell)
iPS	induced pluripotent stem (cell)
PAGE	Polyacrylamide gel electrophoresis
PMSG	Pregnant mare serum gonadotrophin
hCG	Human chorionic gonadotrophin
KSOM	Potassium (Kalium) Simplex optimization medium
Opti-MEM	Reduced-Serum Medium is an improved Minimal Essential Medium

List of Figures

Figure 1	STT formation in mice	29
Figure 2	ETT formation in mice	30
Figure 3	Mouse breeding facilities in Shizuoka University	31
Figure 4	Different mouse strains used in this study	32
Figure 5	<i>MC4R</i> gene editing in the LT strain	33
Figure 6	Pathways for gene edited mouse creation	34
Figure 7	Genotype details of progeny from <i>MC4R</i> genome editing	35
Figure 8	Mouse genotyping techniques for <i>Ter</i> & <i>MC4R</i> genes	36
Figure 9 (i)	A LTXBJ ♀ (90 days old) with normal reproductive system	37
Figure 9 (ii)	Teratoma formation in the double genetically modified strain LT- <i>Ter</i> ^{+/-} / <i>MC4R</i> ^{G25S/G25S}	37
Figure 10	Morphologies of teratomas found in two specimens of LT- <i>Ter</i> ^{-/-} / <i>MC4R</i> ^{G25S/G25S} strains	38
Figure 11	Morphologies of teratomas found in LT- <i>MC4R</i> ^{G25S/G25S} , LT- <i>Ter</i> ^{+/+} / <i>MC4R</i> ^{G25S/G25S} and LT- <i>Ter</i> ^{+/-} / <i>MC4R</i> ^{G25S/G25S} strains	39
Figure 12	Teratoma formation in the knock-in strain LT- <i>MC4R</i> ^{G25S}	40
Figure 13	Morphologies of teratomas in LT- <i>ett1</i> ^{-/-} , LT- <i>Ter</i> ^{+/+} / <i>ett1</i> ^{-/-} & LT- <i>Ter</i> ^{+/-} / <i>ett1</i> ^{-/-} strains	41
Figure 14	Incidence of ovarian teratoma formation in various strains	42
Figure 15	Parthenogenesis of oocytes in the <i>MC4R</i> knock-in strain	43
Figure 16	<i>MC4R</i> expression in oocytes	44
Figure 17	Morphologies of kidney abnormalities found in LT- <i>Ter</i> ^{+/-} / <i>MC4R</i> ^{G25S/G25S} and LT- <i>Ter</i> ^{+/+} / <i>MC4R</i> ^{G25S/G25S} mice strains	45
Figure 18	Morphologies of spleen abnormalities found in, LT- <i>Ter</i> ^{-/-} / <i>MC4R</i> ^{G25S/G25S} , LT- <i>Ter</i> ^{+/-} / <i>MC4R</i> ^{G25S/G25S} and LT- <i>MC4R</i> ^{G25S/G25S} mice strains	46
Figure 19	Morphologies of testis comparing wild, heterozygous, and homozygous type in <i>Ter</i> mutation of LT- <i>Ter</i> / <i>MC4R</i> ^{G25S} and 129/Sv mice strains	47

Chapter 1 Introduction

Teratoma is a tumor containing three germ layer tissues originating from germ cells. Formation of teratoma is reported in humans, monkey (Kawano *et al.*, 2003), rat (Northrup *et al.*, 2012) and birds in addition to mice which are most using animal model for teratoma study. Teratoma are mostly confined within the genital organs and tailbone of the children (Davies *et al.*, 2012). Teratoma in other organs are rarely reported with certain exception for example, teratoma in the pharynx of the newborn (Varras *et al.*, 2009). Teratoma can be occurred naturally or induced experimentally (Stevens, 1964) by transplanting differentiated pluripotent cells (EC cells, ES cells, iPS cells) in an undifferentiated state. These cells have the potential to differentiate into tissues from all three germ layers (Thomson *et al.*, 1998; Takahashi & Yamanaka, 2006). Teratoma also transplantable *i.e.*, parts of teratoma containing pluripotent cells if transplanted teratoma can be formed (Fekete & Ferrigno, 1952). Teratomas can be induced by xenografting human pluripotent stem cells (Damjanov & Andrews, 2007).

In mouse both testicular and ovarian teratomas have been recorded. Mouse testicular teratomas was first reported by Stevens and Little in 1954 (Stevens & Little, 1954). Ovarian teratoma first reported probably in 1920 by Slye. Thiery reported two cases of ovarian teratoma in mice (Thiery, 1963). Till then various cases have been reported but reasons behind teratoma formation was unclear. In this dissertation we enlighten one of the possible reasons for ovarian teratoma formation in mice form molecular point of view.

To distinguish naturally induced teratomas from experimentally induced teratomas, we referred to them as spontaneous testicular teratomas (STT) and experimental testicular teratomas (ETT), respectively (Fig 1 & 2). In a general naked eye both testicular and ovarian teratoma can be observed compared to the normal ones. Furthermore, the tissue section image shows that the tissues derived from three germ layers are mixed. This teratoma can be divided into (benign) teratoma and teratocarcinoma. Both are tumors containing the three-germ layer tissues, while teratoma consists of tissues and cells all differentiated, whereas teratocarcinoma consists of differentiated tissue mass and stem cells that supply them. This stem cell is called an embryonal carcinoma (EC) cell, and it is called teratocarcinoma (malignant teratoma) together with the EC cell and the differentiated three-germ layer cell mass. When differentiation of EC cells is restricted and self-reproductive cycle is repeated, it is called embryonal carcinoma. When this

EC cell is injected into the inner cell mass at the blastocyst stage, a chimeric mouse can be generated.

The strongest candidate gene in the teratoma locus (*Ter*) responsible for testicular teratoma formation was identified as *Dead end 1 (dnd1)* gene. *Dnd1* is a germ plasm-specific maternal RNA and it is expressed in germline of different vertebrate classes, which originally discovered in zebrafish and later in other vertebrates including human, chicken, *Xenopus* and mouse (Weidinger *et al.*, 2003). *Dnd1* has been identified and characterized as germ cell marker in various vertebrates' group. *Dnd1* protein is essential for migration and motility of primordial germ cells (PGCs), only cells destined to transfer genetic information to offspring. PGCs arise far from somatic cells of developing gonads and they must migrate to their site of function. Migration of PGCs follows complex path by various developing tissues as their disruption impacts on the fertility. In 2013, essentiality of *dnd1* for embryonic viability was determined in mice by Zechel (Zechel *et al.*, 2013). In mice, it is colocalized with *nanos2* in P-bodies (Suzuki *et al.*, 2016). However, mutation in mouse *dnd1* did not prevent the formation of PGCs and *Ter* mutation in *dnd1* of mouse, led to loss of germ cells and testicular germ cell cancer (Youngren *et al.*, 2005); therefore, indicating a preserved role of *dnd1* in the development of vertebrates' germline.

In mice, *Dnd* known as *Dnd* microRNA-mediated repression inhibitor 1 (*Dnd1*) which is the zebrafish ortholog of *dnd* and the strongest candidate gene in the teratoma locus *Ter*. *Dnd1* was first recognized on chromosome 18 in the strain 129P3 (The Jackson Laboratory, 2020). A single C to T base change created a stop codon at arginine residue 178 (p.R178X) or 190 (p.R190X) depending on the isoform. The mutation was found only in mice carrying *Ter*, but not in 129 substrains (129T2/SvEmsJ, 129S1/SvImJ, 129X1/SvJ) or other inbred strains (A/J, C57BL/6J, C3H/HeJ and MOLF/Ei). The base change introduces a new *DdeI* restriction enzyme site within the *Dnd1* sequence enabling mice with the *Ter* allele to be distinguished from wild type (Youngren *et al.*, 2005).

The strain 129/Sv, which is genetically susceptible to testicular teratoma production, The STT generating ratio is 1-7 % in the 129 sublimes but almost 100 % in 129/Sv-*Ter* (*Ter/Ter*) mice (Stevens, 1975; Noguchi & Noguchi, 1985). STT formation rather than 129 strain is very rare, excepted one case was reported about ICR mouse in 1997 (Tani *et al.*, 1997). *Ter* congenic mice (B6-*Ter*, LT-*Ter* and C3H-*Ter*) do not generate STT but show the phenotype of PGC loss (Noguchi & Noguchi, 1985). However, experimental testicular teratoma generation can be

induced in 129/Sv (*Ter/Ter*) sublines by transplanting E12.5 fetal testes into adult testes (Stevens, 1964). Experimental testicular teratomas do not require the *Ter* mutation. The mice (129/Sv-*Ter*^{+/+}) that do not generate STT, can produce ETT by transplantation (Noguchi *et al.*, 1996). These results indicate that other genes are responsible for testicular teratoma formation (Jiang & Nadeau, 2001; Sekita *et al.*, 2016).

As same as testis, ovarian teratoma (OT) developed from female germ cells (Stevens & Varnum, 1974; Eppig *et al.*, 1977). Contrary to STT, the molecular mechanisms of OT have been largely unknown. An OT responsible region was reported on chromosome 6, named Ots1, but responsible genes were not yet identified (Lee *et al.*, 1997). However recent molecular genetical approaches demonstrated that OT formation can be induced by various kinds of manipulations on genes regulating activities of follicle cells and oocytes (Yang *et al.*, 2015). Follicle cells and oocytes are under the control of many factors, and changes in the quality and quantity of these factors effect on the regulation of meiotic arrest and apoptosis of oocytes or the activity of follicle cells. Form the series of results, it is expected that mutations in many of these regulatory genes could cause OT.

Previously, we conducted fine mapping on Chrs 18 and 19 for loci associated with generating ETT. Linkage analysis was performed to explore possible candidate genes involved in ETT development using F2 intercross fetuses derived from the F1 of mice susceptible to testicular teratomas, which include the 129/Sv-*Ter*^{+/+} mice (hereafter referred to as 129) and those unsusceptible to testicular teratomas, the LTXBJ mice (hereafter referred to as LT) hybrids. As a result, we identified the locus responsible for ETT formation as “*experimental testicular teratoma 1 (ett1)*” on Chr 18 (Miyazaki *et al.*, 2014).

Additionally, we established LT-*ett1* congenic strains. In these congenic strains, the *ett1* region of the LT is replaced with the corresponding region of the 129 strain, whereas all other chromosomes are derived from the LT strain. Congenic males homozygous for the *ett1* loci were confirmed to form ETTs, indicating that this locus contains the gene responsible for ETTs. The *ett1* locus exists in a region spanning 1.1 Mb (66.3 ~ 67.4 Mb). Eight genes are present in this region. By exome sequencing analysis, we identified a SNP that introduce an amino acid substitution in *MC4R* among these 8 genes (Miyazaki *et al.*, 2018). Since the change was only found in *MC4R*, we interested in this substitution, *MC4R*^{G25S}, as a candidate for ETT responsible gene modification.

In this study, we established a gene edited strain, LT-*MC4R*^{G25S} by using a gene transfer method by electroporation (TAKE method) (Kaneko *et al.*, 2014; Hashimoto & Takemoto, 2015). To introduce single nucleotide exchange (G25S) into *ett1* candidate *MC4R* of LT strain, we designed a set of guide RNAs for CRISPR/Cas9 and ssODN.

As a result, we succeeded to established desired G25S knock-in mouse, LT-*MC4R*^{G25S}, in addition to various mutations in *MC4R*. To explore the roles of *MC4R*^{G25S} in ETT and STT formation, we established LT-*Ter*/*MC4R*^{G25S} by crossing the LT- *MC4R*^{G25S} and LT-*Ter* strains. We also established LT-*Ter*/*ett1* by crossing the LT-*ett1* and LT-*Ter* strains. Surprisingly, highly developed ovarian teratomas (OT) were formed in females in these strains (Figure 9-13). The results demonstrated that *MC4R* is one of the responsible gene for ovarian teratoma formation.

Chapter 2

Materials & Methods

2.1 Mice

129/Sv-*Ter* and LTXBJ mice (Stevens & Varnum, 1974) are gifts from Dr Leroy Stevens (The Jackson Laboratory, Bar Harbor, ME, USA). The 129/Sv-*Ter* (+/+) strain was isolated by Noguchi et al. (Noguchi & Noguchi, 1985) from the STT-sensitive original 129/Sv-*Ter* strain. The STT formation rate of 129 line is 1.4%, while the formation rate of ETT by foetal testes transplantation was 80-90% (Noguchi *et al.*, 1996; Bultman *et al.*, 1992).

The LT males exhibited normal spermatogenesis and generated neither STTs nor ETTs (Noguchi *et al.*, 1996). On the other hand, females of the original LT strain reported to develop almost 100% of OTs from parthenogenetic eggs after sexual maturity (Eppig *et al.*, 1977). The LT strain used as the original strain was established as a strain susceptible to ovarian teratomas, but at the end of 30 years of passage, the current strain has changed so that do not develop OTs at all. At least one and a half years after the establishment of the double-gene-modified strain of LT-*Ter*/MC4R^{G25S}, no OT has been found during the observations over four generations in original LT strain.

The LT-*ett1* congenic strain was established previously and maintained (Miyazaki *et al.*, 2014). The LT-*ett1* strain also exhibited normal spermatogenesis and did not generate STTs but formed ETTs when foetal testes were transplanted into adult testes. In the LT-*ett1* strain, the genome region including the *ett1* locus (which exists at 62.0 - 70.2 Mbp and includes peak markers D18Mit81 and D18Mit184) was substituted with the region from 129/Sv-*Ter* (+/+) mice (Miyazaki *et al.*, 2018).

LT-*Ter* exhibited the germ-cell-loss phenotype in both heterozygous and homozygous mutants. In the LT-*Ter* strain, the genome region including the *ett1* locus (which exists at 33.8 - 46.4 Mbp and includes the *Dnd1* gene) was substituted with the 129/Sv-*Ter* (-/-) region (Sakurai *et al.*, 1995).

The LT-*Ter*/*ett1* double mutant strain was established by crossing these two strains and then back-crossing at least 5 more times with LT-*ett1*.

All these mice were kept and bred under temperature-controlled conditions and had free access to food and water in the animal facilities at Shizuoka University (Fig. 3 & 4). All

animal procedures were performed per the protocols approved by the Institutional Animal Care and Use Committee of Shizuoka University (29A-8, 2018A-19, 2019A-8, 2020A-7).

2.2 Creation of genome-edited mice

In recent years, electroporation gene transfer method (TAKE method) (Kaneko *et al.*, 2014; Hashimoto & Takemoto, 2015) was made the genome editing more easier than the conventional method of injecting fertilized eggs. Therefore, in this study we followed this method to produce genome edited `knock in` mouse for the candidate MC4R gene of *ett1* locus and mutated the 129 strains to the LT strain (G25S) by homologous recombination (Fig. 6).

Using the CRISPR/Cas9 system, a change in a single nucleotide was introduced into the LT strain by using a single-stranded oligodeoxynucleotide (ssODN). As gRNA, two gRNAs sandwiching the target site were selected by CRISPRdirect (<https://crispr.dbcls.jp>) (Fig. 5). An 81-bp ssODN with a 40-bp homologous sequence covering the target region was designed. The synthesis of an ssODN was requested from STAR Oligo (RIKAKEN, Nagoya, Japan). PAGE purification was chosen as the grade of synthesis.

Three days before the day of electroporation, PMSG was administered at 5 IU/100 μ L in the female mice of the LT strain, and one day before, hCG was also administered at a dose of 5 IU/100 μ L per mouse and parity was started.

One hour before egg collection, KSOM medium containing 0.1% hyaluronidase was incubated at 37 °C in a 5% CO₂ incubator to equilibrate the medium. On the day of electroporation, the presence or absence of copulation was confirmed by the presence of a vaginal plug (plug) in female mice. Females with plugs were dissected, a fertilized egg was promptly collected from the ampulla of the fallopian tube, and cumulus cells were removed with KSOM medium containing 0.1% hyaluronidase. The egg from which the cumulus cells were removed was washed four times with KSOM and cultured at 37 °C and 5% CO₂ until electroporation.

Before performing electroporation, KSOM and OPTI-MEM were incubated at 37 °C in a 5% CO₂ incubator to equilibrate the medium. The fertilized eggs that have been cultured were washed three times with OPTI-MEM, and approximately 20 fertilized eggs were transferred to the electrodes so that a small amount of OPTI-MEM was brought into the electrodes for electroporation. Electroporation was performed under the conditions of 25 V, 3 msec ON, 97 msec OFF, and 3 repeats. Eggs transfected with the CRISPR/Cas9 system were immediately collected, washed three times with KSOM, transferred to new KSOM, and

cultured for several hours. A few hours later, the eggs had collapsed, or the parthenogenetic eggs were removed, and the culture was continued until the next day.

On the evening of the electroporation, the ICR strain mouse serving as a host was crossed with a male of the ICR strain that had been subjected to vascular ligation. On the day of transplantation, the presence of a plug in the ICR female was confirmed, and the female with the plug was used as a pseudopregnant mouse host mother. One hour before transplantation, the M2 medium was incubated at 37 °C in a 5% CO₂ incubator to equilibrate the medium.

The fertilization of the eggs cultured from the previous day was confirmed under a microscope. Embryos that had progressed to the 2-cell stage were transferred to M2 medium and prepared for transplantation. The ICR host parent was anaesthetized with 100 µL/10 g body weight of a triple anaesthetic (medetomidine hydrochloride 7.5 µg/L, midazolam 40 µg/µL, butorphanol tartrate 50 µg/µL). The hairs on the left and right dorsal side of the anaesthetized host mother were disinfected with alcohol, and the abdominal wall was incised.

Approximately 15 embryos were aspirated together with a small amount of culture solution with the phases of air, and M2 culture solution was alternately sucked into the glass capillary for embryo transfer at intervals of 2 to 3 mm. The oviduct near the ovary was cut with scissors, a glass capillary was inserted into the fallopian tube, and the embryo was transferred by blowing into the tubule. After transplantation, the fat pad was grasped with tweezers to avoid touching the ovary, the ovary was returned to the body, and the skin was stopped with an autoclip and disinfected with alcohol. The same operation was performed on the other side to complete the embryo transfer operation. After the transplantation, 100 µL of Antisedan (5 mg/mL) was administered per 10 g of body weight, and the temperature was maintained with a heater set at 37 °C until the mouse awakened. Nineteen to 20 days after embryo transfer, litters derived from the transferred embryos were obtained.

2.3 Genotyping

2.3.1 Genotyping for *Ter*

Mouse genomic DNA was extracted by the phenol-chloroform method and the *Ter* target site was amplified by PCR using a primer set (F primer; 5'-TTCCGCCTAATGATGACC, R primer; 5'-CACGTCTGGAATTCACC). The PCR programmed as follows: denaturation at 94 °C for 5 min; 40 cycles of denaturation at 94 °C for 30 sec, annealing at 57 °C for 30 sec; and extension at 72 °C for 40 sec; and extension at 72 °C for 3 min. After amplifying the region containing

the *Ter* mutation, treat it with the restriction enzyme Dde I (TOYOBO) at 37 °C for 2 hours or more, and perform gel electrophoresis. Judgement was made based on the difference in band sizes (for wild type 387bp, 181bp, 97bp and for mutant 356bp, 181bp, 97bp, 31bp). (Fig. 8)

2.3.2 Genotyping for *MC4R*

The tail of a newborn baby or the ear of an adult mouse was removed, genomic DNA was extracted by the phenol-chloroform method, and the *MC4R* target site was amplified by KOD PCR using a primer set (F primer: 5'-CCGAACCCAGAAGAGACCAA, R primer: 5'-GACCCATTTCGAAACGCTCAC). The PCR programmed as follows: denaturation at 94 °C for 5 min; 40 cycles of denaturation at 94 °C for 30 sec, annealing at 67 °C for 30 sec; and extension at 72 °C for 40 sec; and extension at 72 °C for 3 min. The PCR product was electrophoresed on a 1.5% agarose gel. After the confirmation of the PCR product, single-stranded DNA and unreacted dNTPs in the PCR product were inactivated using Illustra ExoStar (GE Healthcare Life Science, Buckinghamshire, UK). An appropriate amount of 40 ng of PCR product, 6.4 pmol of primer, and sterilized water was added to obtain a sample of 14 µL for sequencing. DNA sequencing was outsourced to Fasmac Co., Ltd. The DNA sequence analysis was performed using Codon Code Aligner (<http://www.codoncode.com/aligner/>) and GENETX-MAC (Ver.14.0.3) (Fig. 8).

2.4 Establishment of gene knock-in or knockout strains

Genome-edited mice that could be identified by sequence analysis were back-crossed to LT strain mice. The F1 offspring obtained were also genotyped by sequence analysis and then transferred to sibling mating between the same genotypes. By this way we established Knock-in single mutant LT-*MC4R*^{G25S} strain. Homozygous was obtained by crossing heterozygous male and female mice. After confirming the Homozygous male and female in cross done and later continued to keep the strain. Same procedure was followed to produce homozygous knockout strains LT-*MC4R*⁺² (Fig. 7), LT-*MC4R*^{Δ26} and LT-*MC4R*^{Δ27}.

2.5 Establishment of double mutant mouse strain

We also produce LT-*Ter*^{+/-}/*MC4R*^{G25S/G25S} double mutant strain (Fig. 9) by crossing previously kept LT-*Ter* and newly produced LT-*MC4R*^{G25S} mice strain. LT-*Ter* heterozygous male was crossed with LT-*MC4R*^{G25S} homozygous female. From F1 generation double heterozygous (*Ter*^{+/-}/*MC4R*^{H/G25S}) male and female mice were crossed to produced *Ter*^{+/-}/*MC4R*^{H/G25S} or *Ter*

$^{-}/MC4R^{G25S/G25S}$ mice. The strain was continued by in-crossing with $Ter^{+/-}/MC4R^{H/G25S}$ individuals because double homozygous $Ter^{-}/MC4R^{G25S/G25S}$ male is infertile due to germ cell loss, the notable characteristic of *Ter* mutation.

2.6 Observation of ovarian teratomas

The first OTs was found from one LT- $Ter^{+/-}/MC4R^{G25S}$ female mouse. The mouse abdominal part enlarged and last for over two months. So, the mouse was sacrificed and checked by dissection. After finding the first OTs (Fig. 9), the morphology of the ovaries of each mouse post three months of age was observed and photographed after dissection. Whether the teratoma was developed on both sides or on which side when developed on only one side was recorded. The weight and size of the ovaries were measured. To identify the initial stage of teratoma formation we dissect mice of different stages start from 1-3 months to find parthenogenetic oocyte. (Fig. 15).

2.7 Histological analysis

Tissues were dissected and fixed in Bouin's solution, embedded in paraffin, and serially sectioned at 6- μ m thickness. Deparaffinized sections were stained with Haematoxylin, Eosin and Alcian blue (H-E-A) and screened for the presence of OTs under a light microscope (Fig. 12).

2.8 Immunohistochemical observation

For immunohistochemical observation one month old 3 mice were selected, sacrificed and ovaries collected. Ovaries were then fixed with 4% PFA, dehydrated, cleared, and embedded in paraffin to prepare 5 μ m-thick sections. After deparaffinization, the tissue was surrounded with a liquid blocker, Pap Pen (DAIDO SANGYO CO., LTD, Tokyo Japan). Sections were blocked with 3% BSA/TBST. After 3 washes with TBST for 10 minutes, the primary antibody, anti-MC4R (1:80, Cayman Chemical, 10006355), diluted with 3% BSA/TBST, was reacted overnight at 4 °C. Sections were washed 3 times with TBST for 10 min. Then, the secondary antibody, anti-rabbit IgG (H+L), F(ab')₂ fragment (Alexa Fluor 488 conjugate) (1:500, Cell Signaling, #4412), diluted with 3% BSA/TBST, was reacted at room temperature for 1 hour. After 3 washes with TBST for 10 minutes, sections were enclosed with a water-soluble encapsulant (containing DAPI). As a negative control, MC4R blocking peptide (Cayman Chemical, 10006355) was used to react with primary antibodies. A Carl Zeiss confocal laser scanning microscope (LSM700) was used for fluorescence observation.

In our previous study we identified possible genes (*MC4R* in each *ett1* region, 3 genes in *Poly3c*, *Cd160*, *Pdzk1* in *ett2* region, and *Prmt3* gene in *ett3* region) by linkage analysis and exome sequencing for ETT formation (Miyazaki *et al.*, 2018). Among these genes we conducted genome editing to produce knock-in mice with the *Mc4r* gene because, SNPs in which amino acid substitution (G25S) occurs in 129 gene background only in this gene.

3.1 Creation of genome editing mice

Genome editing to introduce the identified single-nucleotide substitution in *MC4R* of the LT strain to the 129 strain was performed by using the CRISPR/Cas9 system. Two gRNAs (gRNA1, gRNA2) sandwiching the target site were selected by CRISPRdirect (<https://crispr.dbcls.jp>). A ssODN was designed to have a 40 bp homologous sequence at each end of the target site (Fig. 5). TAKE (Technique for Animal Knockout system by Electroporation) was used as an actual introduction method (Kaneko *et al.*, 2014; Hashimoto & Takemoto, 2015). This method does not require the injection of a reagent into a fertilized egg and enables easy genome editing.

In total, 110 2-cell stage embryos that were transfected with the CRISPR/Cas9 system were implanted, resulting in the birth of 13 offspring (11.82%). Among the 13 juveniles, 10 were F0 generation mice in which some mutation was introduced (76.92%). DNA sequence analysis of the F1 generation from the crossing of F0 and wild-type LT strain showed five types of mutations in addition to the desired knock-in mutation to substitute G in LT to A in 129 to induce *MC4R*^{G25S} (Fig. 5). Mutations with a 2 bp insertion (+2), a 1 bp deletion (Δ 1), a 26 bp deletion (Δ 26), and a 27 bp deletion (Δ 27), and a genotype that could not be determined (M), were obtained (Fig. 7). +2, Δ 1, and Δ 26 are mutants that introduce a stop codon due to frameshifting, and Δ 27 causes the deletion of 9 amino acids among two target sites. Homozygous strains for each genotype of +2, Δ 1, Δ 26, Δ 27 and *MC4R*^{G25S} were established. Gene knockout genotype mouse strains +2 (Fig. 7C) along with Δ 1, Δ 26 showed an obese phenotype that indicates *MC4R* deficiency, as reported. In contrast to the knockout mouse, knock-in mouse LT-*MC4R*^{G25S} did not show any obvious phenotype (Fig. 7D). Additionally, LT-*MC4R* ^{Δ 27} did not show an obese phenotype. We maintained lines LT-*MC4R*⁺², LT-*MC4R* ^{Δ 27} and LT-*MC4R*^{G25S} for further analysis. LT-*MC4R* ^{Δ 26}, LT-*MC4R* ^{Δ 1}, LT-*MC4R*^M and strains were later abolished because of same obese phenotype as LT-*MC4R*⁺² (Appendix Table 2).

3.2 Creation of double mutant mice

In addition to ETTs, we attempted to cross LT-*MC4R*^{G25S} and LT-*Ter* mice to address whether the substitution of amino acids in *MC4R* resulted in the formation of STTs. But we did not recognize any STT like the original 129/Sv strain or so. Phenotypically testis of the double homozygous male (*Ter*^{-/-}/*MC4R*^{G25S/G25S}) were smallest in size and weight with germ cell loss compare to the wild type (+/G25S). (Fig. 19A). This characteristic is similar with original 129 (-/-, -/+ and +/+) (Fig. 19B) and other *Ter* congenic mice. This result demonstrates that *MC4R* is not linked with STT formation.

However, we found that some LT-*Ter*/*MC4R*^{G25S} females had swollen abdomens at approximately 3 months old or older. We found highly developed OTs after dissection in both heterozygous (^{+/*Ter*/G25S/G25S}) (Fig. 9) and homozygous (^{*Ter*/*Ter*/G25S/G25S}) mice (Fig. 10). Then, we checked the ovaries of LT-*MC4R*^{G25S} mice. OTs were also found in LT-*MC4R*^{G25S} mice (Fig. 11A). In OTs, various types of tissues of three germ layers, such as neuronal tissue, keratin pearl (ectodermal), adipose tissue (mesodermal), & mucinous glandular structure with ciliated epithelium (endodermal), were observed prior to histological studies (Fig. 12B-F).

3.3 Observation of OTs in other mice strains

Previously we also crossed LT-*Ter* and LT-*ett1* mice to establish an LT-*Ter*/*ett1* double congenic strain to address genetic changes in the *ett1* region in combination with *Ter* mutation, resulting in the formation of STTs.

After establishing the LT-*Ter*/*MC4R*^{G25S} strain, we started to check OTs formation along with another double congenic mutant strain LT-*Ter*/*ett1*. We continued to check both the ovaries and testes of all the strains for searching teratomas. Morphologies of teratomas were photographed and are shown in Figure 13. The incidents of teratoma in each genotype are summarized in Figure 14. Both mouse strains LT-*MC4R*^{G25S/G25S} and LT-*ett1*^{-/-} that possess 129-type *MC4R* developed OTs, but both heterozygous *MC4R*^{G25S/+} and *ett1*^{+/-} mice did not produce OTs even in double-modified or congenic strains. OTs formation rate is 100% for the LT-*Ter*^{-/-}/*MC4R*^{G25S/G25S} individuals (Fig. 10). The incidence of OTs was significantly higher in LT-*ett1*^{-/-} mice (75%) than in LT-*MC4R*^{G25S/G25S} mice (49%). The incidence of OTs was significantly increased to 67% when the *Ter* region was introduced in heterozygous to *MC4R*^{G25S/G25S} mice. In the case of LT-*ett1*^{-/-}, the incidence of OTs was not changed by the introduction of *Ter* but was lowered in LT-*Ter*^{+/-}/*ett1*^{-/-} mice. The incidence of OT formation was significantly decreased in LT-*Ter*^{+/-}/*MC4R*^{G25S/G25S} mice compared with LT-*MC4R*^{G25S/G25S} mice. As

indicated in Appendix Table 1, the small region of chromosome 18 identified by the D18Mit84 marker was introduced into LT. Thus, even in LT-*Ter*^{+/+}, a small fragment of the 129 strain was inserted. There is a possibility that other genes that promote teratoma formation exist in this region. Almost same type of result has been observed from the double congenic strain, where OTs incidence was lower in LT-*Ter*^{+/+}/*ett1*^{-/-} (47%) than in LT-*ett1*^{-/-} mice (75%). It remains constant in case of the single mutant strains too by showing OTs incidence was significantly lower in LT-*MC4R*^{G25S/G25S} than LT-*ett1*^{-/-} mice. These results suggested that the *ett1* region contains the responsible genes that can promote OT formation rather than *MC4R*. Additionally, the predicted genes in the D18Mit84 region and the *ett1* region might have competitive effects on each other. No OT formation was founded in the original strain LT or in mutants of *MC4R* (+2, Δ 26 & Δ 27).

3.4 Search for parthenogenesis from the Knock-in mouse ovary

Ovarian teratomas have been known to develop from the parthenogenesis of oocytes (Furuta *et al.*, 1995; Hirao & Eppig, 1997). Thus, we tried to check this by observing sections prepared from mice that were expected to start to produce teratomas. We prepared sections of ovaries from one-month-old mice. As expected, oocytes divided into 2 cells in the small follicle were found in knock-in LT-*MC4R*^{G25S/G25S} mice (Fig. 15). It is suggested that these 2 cells are produced by the parthenogenesis of the oocyte. On an average 2 parthenogenetic oocytes were observed in a single ovary.

3.5 Immunohistochemistry of Knock-in mouse ovary

Immunohistochemical analysis showed that MC4R protein was expressed in the oocytes of knock-in LT-*MC4R*^{G25S/G25S} female ovary while not in the knockout LT-*MC4R*^{+2/+2} (Fig. 16). This result is an indication of our successful genome editing mice creation.

3.6 Observation of abnormalities in other organs of Knock-in mice

During study we observed abnormalities in kidney (Fig. 17) and spleen (Fig. 18) too in LT-*Ter*/*MC4R*^{G25S} double mutant mice. Kidney formed robust pale colour, fluid filled structure and the occurrence percentage is higher in male than female. We also find abnormal spleen where it elongated, robust and darkish colour. Reversely abnormalities occurrence in spleen is higher in females than the males. This result is jump to 100% in case of LT-*Ter*^{-/-}/*MC4R*^{G25S/G25S} individuals suggesting a correlation with OTs formation. This study is now in proceeding to get

a steady result with more replications. No such abnormalities confirmed from in other strains except knock-in individuals.

Discussions

Teratoma is an important tool for stem cell research (Nelakanti *et al.*, 2016). There is shortage of information about the origin of teratoma from the molecular level. So, in this study we try to elucidate about the origin of teratoma. Previously we introduced the *Ter* gene, which is one of the causative genes for teratoma formation found in 129 strains that develop STTs and ETTs, into LT strains that do not develop STTs and ETTs. A single-nucleotide substitution was introduced into the *MC4R* gene to introduce the same amino acid substitution as in the 129 strain. The introduction of the *Ter* gene resulted in a germ-cell-loss phenotype in both males and females, as in the case of the *Ter*-gene-introduced lines produced from other lines (Noguchi, 1996). Then, it was revealed that the *Ter* gene product DND1 is essential for germ cell formation and that other genes are also necessary for the onset of teratomas. We mapped the *ett1* region, which is a candidate region for ETTs, and found a SNP in the *MC4R* gene that causes an amino acid change between the 129 strains and the LT strains among the 8 genes existing in the *ett1* region (Miyazaki *et al.*, 2018). Thus, the single amino acid change in the *MC4R* gene is supposed to be a candidate for *ett1*. Then, to identify the *ett1* gene, a knock-in strain, LT-*MC4R*^{G25S}, in which this single base substitution was introduced into the LT strain, was created by genome editing. By crossing this knock-in line with the LT-*Ter* line, we tried to investigate the possibility of developing STTs or ETTs due to the combined effect of *Ter* and *MC4R*^{G25S}. Surprisingly, highly developed OTs developed at an extremely high rate in the double mutant strain LT-*Ter*/*MC4R*^{G25S} (approximately 75% to 100% respectively). The original LT strain was established as a susceptible strain for OTs, but at the end of 30 years of passage, the current strain has changed so that OTs do not develop at all. At least one and a half years after the establishment of the double-gene-modified strain of LT-*Ter*/*MC4R*^{G25S} mice, no case of OTs was found during the observations over four generations. Thus, we introduced two candidate teratoma-causing genes into a line that does not develop OTs and analysed their combined effects. From many years of research so far, the mechanism of ovarian teratoma development is that some of the germ cells begin parthenogenesis for some reason in the process of germ cell apoptosis (Eppig *et al.*, 1977). Our results suggest that *MC4R* is involved in the regulation of germ cell apoptosis and that changes in the *MC4R*-mediated signal transduction system cause germ cell parthenogenesis. Because we also observed parthenogenesis in the prior to ovarian teratoma formation in the ovary of our knock-in *MC4R*^{G25S} mutant strain mice.

The melanocortin 4 receptor (*MC4R*) gene is involved in energy intake and energy expenditure (Kublaoui *et al.*, 2006); energy homeostasis (Füredi, N. *et al.* 2017). *MC4R* coupled with stimulating G protein (Gs) promotes protein kinase A (PKA) activation and induces cAMP production. The signal transduction pathway through *MC4R* suppresses c-Jun N-terminal kinase (JNK) (Tao, 2010). From the results of *MC4R* gene targeting, it is well known that *MC4R*-gene-deficient mice become obese, and the *MC4R* gene is deeply involved in energy control (Huszar *et al.*, 1997). MSH, agouti and agouti-related protein (AGRP) are known as ligands for *MC4R* (Yang & Tao, 2016). 129/Sv-Ay^(Ay/+) male mice are known to have a 10-fold lower rate of testicular teratoma formation than wild-type mice (Stevens, 1967). Ay is a dominant mutation in the agouti gene and causes ectopic expression of agouti protein and the inhibition of *MC1R* and *MC4R* chronic signal transduction systems (Bultman *et al.*, 1992; Dinulescu & Cone, 2000; Miller *et al.*, 1993). As an agonist of *MC4R*, agouti-related (AGRP) has been found to be a related gene of agouti, and it has been reported that AGRP has a 100-fold higher binding affinity to *MC4R* than agouti (Fong *et al.*, 1997). According to the docking model of *MC4R* and its ligand, the binding of AGRP and *MC4R* involves the N-termini of *MC4R* K33, Y35 and D37, and the binding of MSH and *MC4R* does not involve the N-terminus of *MC4R* (Heyder *et al.*, 2019). From this, it can be

speculated that the ligand of *MC4R* in the development of ovarian teratomas in this double-gene-modified line is AGRP. Additionally, the G25S missense mutation of *MC4R* inhibits the binding to AGRP, which suppresses the action of the *MC4R* antiapoptotic signal. As indicated in this study, *MC4R* protein is expressed in mouse oocytes. It is hypothesized that the modification of the antiapoptotic pathway of oocytes is relatively enhanced to increase the rate of parthenogenesis and cause ovarian teratoma formation.

Detailed analysis of the function of *DND1* identified as the *Ter* gene is underway. Yamaji *et al.* indicated that *DND1*-dependent mRNA destabilization is required for the survival of mouse PGCs and spermatogonial stem cells by suppressing apoptosis (Yamaji *et al.*, 2017). By contrast, there is a report that showed that *DND1* protects and maintains germ cell fate (Gross-Thebing *et al.*, 2017). *DND1*-deficient germ cells transdifferentiate into somatic cells. The translation of *nanos1*, a determinant of germ cells, requires *DND1* (Aguero *et al.*, 2017; 2018). Recently, it was demonstrated that *Nanos2* and *Nanos3* are involved in testicular teratoma formation by establishing a double mutant strain with each gene and *Ter* (Imai *et al.*, 2020). Thus, a loss-of-function mutation in *DND1* is essential for teratoma formation.

Although the DND1 gene was identified as being essential for testicular teratoma formation, no specific gene was reported for ovarian teratomas. The OT-related locus was reported previously; however, a mutated gene in the locus has not yet been identified (Lee *et al.*, 1997). However, the genes suggested to be responsible for OTs were found with gene knockout approaches. As a result of the generation of many genetically modified mice so far, it has been reported that ovarian teratomas also develop by different mechanisms. The onset of OTs due to parthenogenesis has been reported in mice in which the *Mos* gene has been knocked out, which has the function of meiotic arrest. Yang *et al.* showed that conditional knockout mice of retinoblastoma protein 1 (*Rb1*) developed ovarian teratomas and that abnormalities of somatic follicular cells also cause teratoma formation (Yang *et al.*, 2015). Similarly, the overexpression of *Bcl-2*, constitutive active mutation in the FSH receptor, a missense mutation in *Foxo3a* and the knockout of the *Tgkd* gene are other examples of teratoma formation caused by somatic abnormalities and the genetic background of mouse strains (Hsu *et al.*, 1996; Peltoketo *et al.*, 2010; Youngson *et al.*, 2011; Balakrishnan & Chaillet, 2013). Although the mechanism of teratoma formation is unknown, global knockdown of the *Gata4* gene by siRNA also induced the formation of OTs (Thurisch *et al.*, 2009). Recently Batarfi *et al.*, (2019) mentioned that two of *MC4R* variants s12970134 and rs17782313 are associated with obese polycystic ovary syndrome patients. Various group worldwide work with ovarian teratomas using different model animals, also with human. But none of them reported about the mechanism from molecular point of view clearly due to complex approach of OTs. In this way, it has become clear that there is an onset mechanism caused by germ-cell-derived teratomas and somatic cells. Many gene mutations can cause teratomas because the formation and divisional control of germ cells are performed under complicated control of the follicular cells covering them and growth factors in the ovary. To elucidate the whole picture of the mechanism of teratoma formation, it is necessary to analyse it at the whole-genome level.

The *LT-Ter/MC4R^{G25S}* double-gene-modified line we established was used to elucidate the cause of testicular teratomas. Until now no STT was recorded as 129/Sv strain. Morphologically the size of the testis of *LT-Ter^{-/-}/MC4R^{G25S/G25S}* is smaller than the *LT-Ter^{-/+}/MC4R^{G25S/G25S}* and *LT-Ter^{+/+}/MC4R^{G25S/G25S}* individuals as like as other *Ter* congenic and original 129/Sv strains. This result is constant as all the male of *LT-Ter/MC4R^{G25S}* strain demonstrated same morphological characteristics while, the knock-in single mutant *LT-MC4R^{G25S}* resembles as wild type.

During study alongside the OTs we also observed other organs. Surprisingly, we found abnormalities in kidney and spleen too in *LT-Ter/MC4R^{G25S}* double mutant mice. Kidney formed robust pale colour; fluid filled structure. This occurrence is higher in male than female. We also find abnormal spleen where it elongated, robust and darkish color. This study is now in proceeding. No such abnormalities confirmed from in other strains except some knock-in individuals. Teratoma of kidney is an exceptionally rare case as we knew that teratomas are predominantly embryonal origin (Glazier *et al.*, 1980). Teratoma of kidney was first reported by Mc Curdy in 1934 (Liu *et al.*, 2000). In 2009, Nirmal *et al.*, reported about primary intrarenal teratoma formation in an adult female. So far kidney teratoma study was confined with the human cases only and not more than 30 cases were reported. In 2013, Aldahmash *et al.* reported that ESCs can form teratomas in immunocompetent mice after allogeneic as well as syngeneic implantation. Spontaneous kidney teratoma formation in mice or another model organism were not reported yet. Our study is under investigation whether these abnormalities for extragonadal organs are originated from teratoma or not and there are any relations with *MC4R* gene with these abnormalities.

References

- Aguero, T. *et al.* Maternal *Dead-end 1* promotes translation of *nanos1* by binding the eIF3 complex. *Development* **144**, 3755-3765, doi:10.1242/dev.152611 (2017).
- Aguero, T. *et al.* Combined functions of two RRM domains in *Dead-end1* mimic helicase activity to promote *nanos1* translation in the germline. *Molecular Reproduction and Development* **85**, 896-908, doi:10.1002/mrd.23062 (2018).
- Aldahmash *et al.* Teratoma formation in immunocompetent mice after syngeneic and allogeneic implantation of germline capable mouse embryonic stem cells. *Asian Pac J Cancer Prev* **14**(10), 5705-5711 (2013).
- Balakrishnan, A. & Chaillet, J. R. Role of the inositol polyphosphate-4-phosphatase type II *Inpp4b* in the generation of ovarian teratomas. *Dev Biol* **373**, 118-129, doi:10.1016/j.ydbio.2012.10.011 (2013).
- Batarfi, *et al.* MC4R variants rs12970134 and rs17782313 are associated with obese polycystic ovary syndrome patients in the Western region of Saudi Arabia. *BMC Medical Genetics*, **20**, 144 (2019).
- Bultman, S. J., Michaud, E. J. & Woychik, R. P. Molecular characterization of the mouse agouti locus. *Cell* **71**, 1195-1204, doi:10.1016/s0092-8674(05)80067-4 (1992).
- Damjanov, I. & Andrews, P. W. Teratomas produced from human pluripotent stem cells xenografted into immunodeficient mice – a histopathology atlas. *Nat Biotechnol* **25**, 1-44 (2007).
- Davies, M., Inglis, G., Jardine, L. and Koorts, P. *Antenatal Consults: A Guide for Neonatologists and Paediatricians – E-Book*. Elsevier Health Sciences. P. 298 (2012).
- Dinulescu, D. M. & Cone, R. D. Agouti and agouti-related protein: analogies and contrasts. *J Biol Chem* **275**, 6695-6698 (2000).
- Eppig, J. J., Kozak, L. P., Eicher, E. M. & Stevens, L. C. Ovarian teratomas in mice are derived from oocytes that have completed the first meiotic division. *Nature* **269**, 517-518, doi:10.1038/269517a0 (1977).
- Fekete, E. & Ferrigno, M. A. Studies on a transplantable teratoma of the mouse. *Cancer Res* **12**, 438-440 (1952).

- Fong, T. M. *et al.* ART (protein product of agouti-related transcript) as an antagonist of MC-3 and MC-4 receptors. *Biochem Biophys Res Commun* **237**, 629-631, doi:DOI 10.1006/bbrc.1997.7200 (1997).
- Füredi, N. *et al.* Melanocortin 4 receptor ligands modulate energy homeostasis through urocortin 1 neurons of the centrally projecting Edinger-Westphal nucleus. *Neuropharmacology* **118**, 26-37 (2017)
- Furuta, Y. *et al.* Ovarian Teratomas in Mice Lacking the Protooncogene C-Mos. *Jpn J Cancer Res* **86**, 540-545, doi:DOI 10.1111/j.1349-7006.1995.tb02432.x (1995).
- Glazier, W. B., Lytton, B. and Tronic, B. Renal teratomas: case report and review of the literature. *J Urol* **123**, 98-99 (1980).
- Gross-Thebing, T. *et al.* The Vertebrate Protein Dead End Maintains Primordial Germ Cell Fate by Inhibiting Somatic Differentiation. *Dev Cell* **43**, 704+, doi:10.1016/j.devcel.2017.11.019 (2017).
- Hashimoto, M. & Takemoto, T. Electroporation enables the efficient mRNA delivery into the mouse zygotes and facilitates CRISPR/Cas9-based genome editing (vol 5, 11315, 2015). *Sci Rep-Uk* **5**, doi:ARTN 12658, doi:DOI 10.1038/srep12658 (2015).
- Heyder, N. *et al.* Signal Transduction and Pathogenic Modifications at the Melanocortin-4 Receptor: A Structural Perspective. *Front Endocrinol* **10**, doi:ARTN 515, doi:DOI 10.3389/fendo.2019.00515 (2019).
- Hirao, Y. & Eppig, J. J. Parthenogenetic development of Mos-deficient mouse oocytes. *Mol Reprod Dev* **48**, 391-396, doi:10.1002/(SICI)1098-2795(199711)48:3<391::AID-MRD13>3.0.CO;2-Z (1997).
- Hsu, S. Y., Lai, R. J. M., Finegold, M. & Hsueh, A. J. W. Targeted overexpression of Bcl-2 in ovaries of transgenic mice leads to decreased follicle apoptosis, enhanced folliculogenesis, and increased germ cell tumorigenesis. *Endocrinology* **137**, 4837-4843, doi:DOI 10.1210/en.137.11.4837 (1996).
- Huszar, D. *et al.* Targeted disruption of the melanocortin-4 receptor results in obesity in mice. *Cell* **88**, 131-141 (1997).
- Imai, A. *et al.* Mouse *dead end1* acts with *Nanos2* and *Nanos3* to regulate testicular teratoma incidence. *PLoS One* **15**, e0232047, doi:10.1371/journal.pone.0232047 (2020).

- Jiang, L. I. & Nadeau, J. H. 129/Sv mice--a model system for studying germ cell biology and testicular cancer. *Mamm Genome* **12**, 89-94 (2001).
- Kaneko, T., Sakuma, T., Yamamoto, T. & Mashimo, T. Simple knockout by electroporation of engineered endonucleases into intact rat embryos. *Sci Rep-Uk* **4**, doi:ARTN 6382, doi:DOI 10.1038/srep06382 (2014).
- Kawano, K. *et al.* Mature ovarian teratoma in a Cynomolgus Monkey (*Macaca fascicularis*). *J Toxicol Pathol* **16**, 283-185 (2003).
- Kublaoui, B. M., Holder, J. L., Jr., Tolson, K. P., Gemelli, T. & Zinn, A. R. SIM1 overexpression partially rescues agouti yellow and diet-induced obesity by normalizing food intake. *Endocrinol* **147**, 4542-4549 (2006).
- Lee, G. H. *et al.* Genetic dissection of susceptibility to murine ovarian teratomas that originate from parthenogenetic oocytes. *Cancer Res* **57**, 590-593 (1997).
- Liu, Y. C. *et al.* Intrarenal mixed germ cell tumor. *J Urol* **164**, 2020-2021 (2000).
- Miller, M. W. *et al.* Cloning of the mouse agouti gene predicts a secreted protein ubiquitously expressed in mice carrying the lethal yellow mutation. *Genes Dev* **7**, 454-467 (1993).
- Miyazaki, T. *et al.* Identification of genomic locus responsible for experimentally induced testicular teratoma 1 (*ett1*) on mouse Chr 18. *Mamm Genome* **25**, 317-326, doi:10.1007/s00335-014-9529-8 (2014).
- Miyazaki, T. *et al.* Identification of Two Additional Genomic Loci Responsible for experimentally induced testicular teratoma 2 and 3 (*ett2* and *ett3*). *Zool Sci* **35**, 172-178, doi:10.2108/zs170176 (2018).
- Nelakanti, *et al.* Teratoma Formation: A Tool for Monitoring Pluripotency in Stem Cell. *Curr. Protoc. Stem Cell Biol* **32**, 4A. 8. 1-4A. 8. 17. Doi: 10.1002/9780470151808.Sc04a08s32 (2016).
- Nirmal, T. J., Krishnamoorthy, S. and Korula, A. Primary intrarenal teratoma in adult: A case report and review of literature. *Indian J Urol* **25**(3), 404-406 (2009).
- Noguchi, T. & Noguchi, M. A recessive mutation (*Ter*) causing germ cell deficiency and a high incidence of congenital testicular teratomas in 129/Sv-ter mice. *J Natl Cancer Inst* **75**, 385-392 (1985).
- Noguchi, M. *et al.* The *ter* mutation responsible for germ cell deficiency but not testicular nor

- ovarian teratocarcinogenesis in *ter/ter* congenic mice. *Develop Growth Differ* **38**, 59-69 (1996).
- Northrup, E. *et al.* The *ter* mutation in the Rat *Dnd1* gene initiates gonadal teratomas and infertility in both genders. *PLoS One* **7**(5), 1-13 (2012).
- Peltoketo, H. *et al.* Female mice expressing constitutively active mutants of FSH receptor present with a phenotype of premature follicle depletion and estrogen excess. *Endocrinology* **151**, 1872-1883, doi:10.1210/en.2009-0966 (2010).
- Sakurai, T., Iguchi, T., Moriwaki, K. & Noguchi, M. The *ter* mutation first causes primordial germ cell deficiency in *ter/ter* mouse embryos at 8 days of gestation. *Develop Growth Differ* **37**, 293-302 (1995).
- Sekita, Y., Nakamura, T. & Kimura, T. Reprogramming of germ cells into pluripotency. *World J Stem Cells* **8**, 251-259, doi:10.4252/wjsc.v8.i8.251 (2016).
- Slye, M., Holmes, H. F. and Wells, H. G. *J Cancer Res* **5**, 205 (1920).
- Stevens, L. C. & Little, C. C. Spontaneous Testicular Teratomas in an Inbred Strain of Mice. *Proc Natl Acad Sci U S A* **40**, 1080-1087 (1954).
- Stevens, L. C. & Varnum, D. S. The development of teratomas from parthenogenetically activated ovarian mouse eggs. *Dev Biol* **37**, 369-380 (1974).
- Stevens, L. C. Experimental Production of Testicular Teratomas in Mice. *Proc Natl Acad Sci U S A* **52**, 654-661 (1964).
- Stevens, L. C. Teratocarcinogenesis and spontaneous parthenogenesis in mice. *Symp Soc Dev Biol*, 93-106 (1975).
- Stevens, L. C. The biology of teratomas. *Adv Morphog* **6**, 1-31 (1967).
- Suzuki, A. *Dead end1* is an essential partner of *NANOS2* for selective binding of target RNAs in male germ cell development. *EMBO Rep* **16**, 1-10 (2016).
- Tani, *et al.* Spontaneous testicular teratoma in an ICR mouse. *Toxicologic Pathology*, **25**(3), 317-320 (1997).
- Tao, Y. X. The Melanocortin-4 Receptor: Physiology, Pharmacology, and Pathophysiology, doi:DOI 10.1210/er.2009-0037. *Endocrine Reviews* **31**, 506-543 (2010).

- Takahashi, K. and Yamanaka, S. Induction of pluripotent stem cells from mouse embryonic and adult fibroblast cultures by defined factors. *Cell* **126**, 663-676 (2006).
- The Jackson Laboratory. *129T1/Sv-Oca2⁺ Tyr^{c-ch} Dnd1^{Ter}/J*, 16th December 2020 (2020). (<https://www.jax.org/strain/000091>)
- Thiery, M. Ovarian teratoma in the mouse. *Br J Cancer* **17**, 231-234 (1963).
- Thomson, J. A. *et al.* Embryonic stem cell lines derived from human blastocysts. *Science* **282**, 1145-1147 (1998).
- Thurisch, B. *et al.* Transgenic mice expressing small interfering RNA against *Gata4* point to a crucial role of *Gata4* in the heart and gonads. *J Mol Endocrinol* **43**, 157-169, doi:10.1677/JME-09-0030 (2009).
- Varras, M., Akrivis, C., Plis, C. and Tsoukalos, G. Antenatal sonographic diagnosis of pharyngeal teratoma: our experience of a rare case with review of the literature. *Obstet Gynecol Int* **2009**, 1-4 (2009)
- Weidinger, G. *et al.* *Dead end*, a novel vertebrate germ plasm component, is required for zebrafish primordial germ cell migration and survival. *Curr Biol* **13**, 1429–1434 (2003).
- Yamaji, M. *et al.* *Dnd1* maintains germline stem cells via recruitment of the CCR4-NOT complex to target mRNAs. *Nature* **543**, 568-572, doi:10.1038/nature21690 (2017).
- Yang, Q. E., Nagaoka, S. I., Gwost, I., Hunt, P. A. & Oatley, J. M. Inactivation of Retinoblastoma Protein (Rb1) in the Oocyte: Evidence That Dysregulated Follicle Growth Drives Ovarian Teratoma Formation in Mice. *Plos Genet* **11**, doi:ARTN e1005355 (2015)
- Yang, Z. & Tao, Y. X. Biased signaling initiated by agouti-related peptide through human melanocortin-3 and-4 receptors. *Bba-Mol Basis Dis* **1862**, 1485-1494, doi:10.1016/j.bbadis.2016.05.008 (2016).
- Youngren, K. K. The *Ter* mutation in the *dead end* gene causes germ cell loss and testicular germ cell tumours. *Nature* **435**, 360–364 (2005).
- Youngson, N. A. *et al.* A missense mutation in the transcription factor *Foxo3a* causes teratomas and oocyte abnormalities in mice. *Mamm Genome* **22**, 235-248, doi:10.1007/s00335-011-9317-7 (2011).

Zechel, J. L. Contrasting effects of Deadend1 (*Dnd1*) gain and loss of function mutations on allelic inheritance, testicular cancer, and intestinal polyposis. *BMC Genet* **14**(54), 1-10 (2013).

Figures



Normal Testis

STT

Figure 1: STT formation in mice.

Normal testis (Upper left) and Spontaneous testicular teratoma (STT) (Upper right) formed in Sv/129 lines. Histology of normal testis (Lower left) showing nicely arranged and STT (lower right) showing different tissues rather than normal including Bone (B), cartilage (C), secretory epithelium (se), neural tube (Nt).

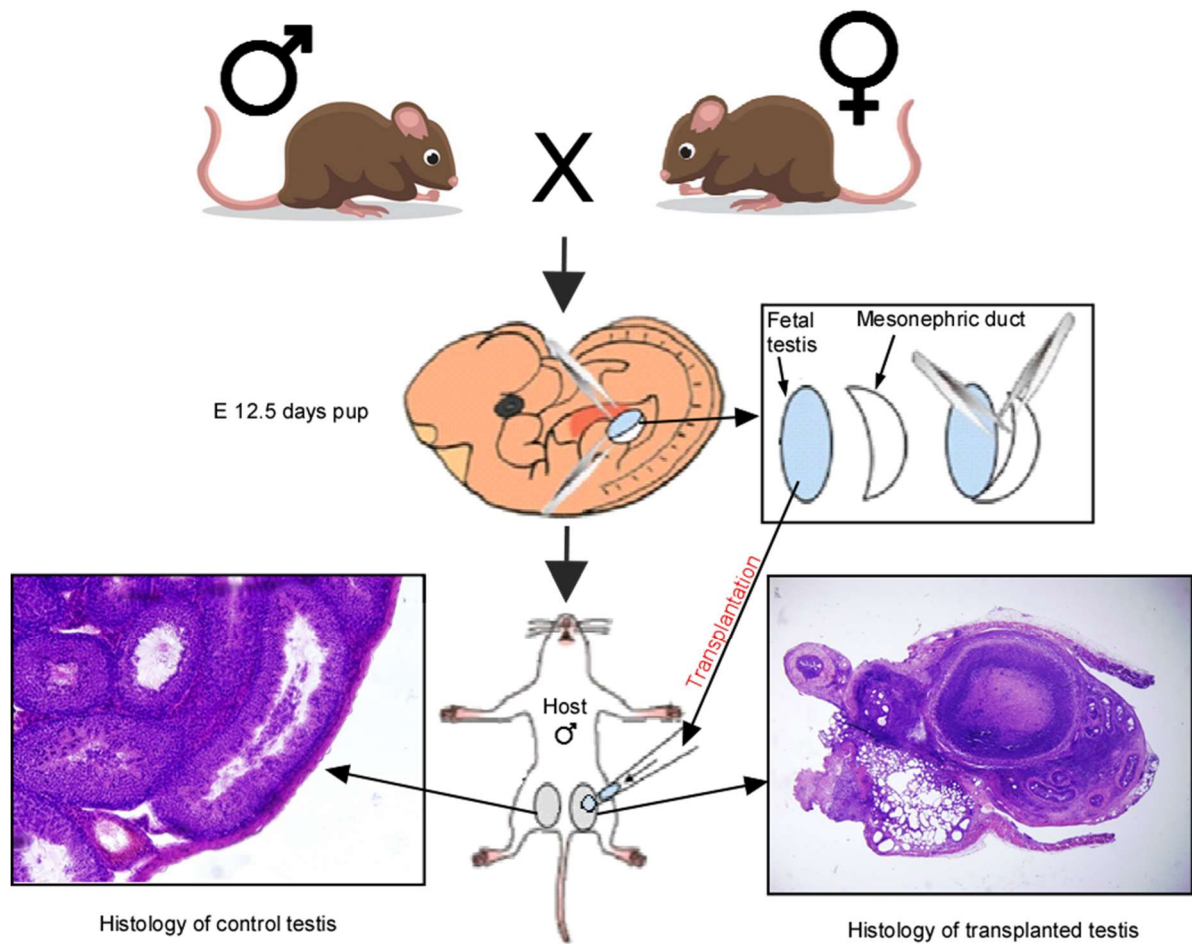


Figure 2: ETT formation in mice.

Diagram of experimental testicular teratoma (ETT) by fetal testis transplantation. Two months old male and female were paired and after 12.5 days fetal testis was transplant into one testis of the host while another was kept as control or without transplantation. After 1 months of surgery host was sacrificed and testis were prepared for histological observation to find ETT and compare with control.



Figure 3: Mouse breeding facilities in Shizuoka University.

Mouse breeding and care house, animal facilities division, Department of Science, Shizuoka University (upper photo). Inside mouse room (lower photo).

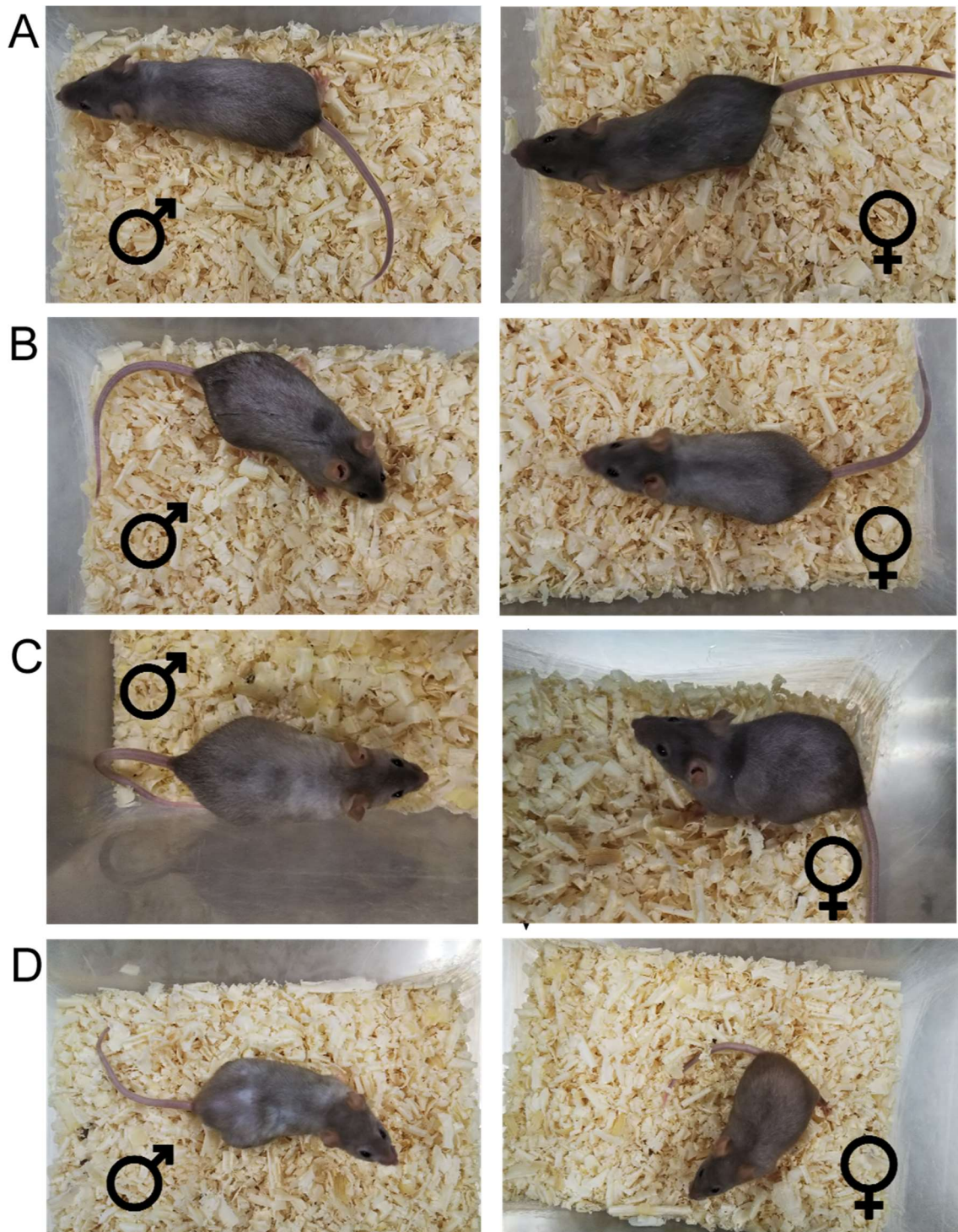
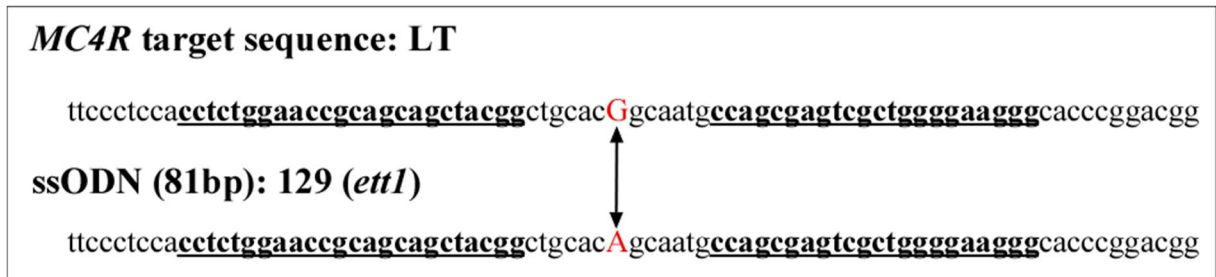


Figure 4: Different mouse strains used in this study.

(A) LTXBJ, (B) *LT-Ter*, (C) *LT-ett1* and (D) *LT-Ter/ett1* mice.

A.



B.

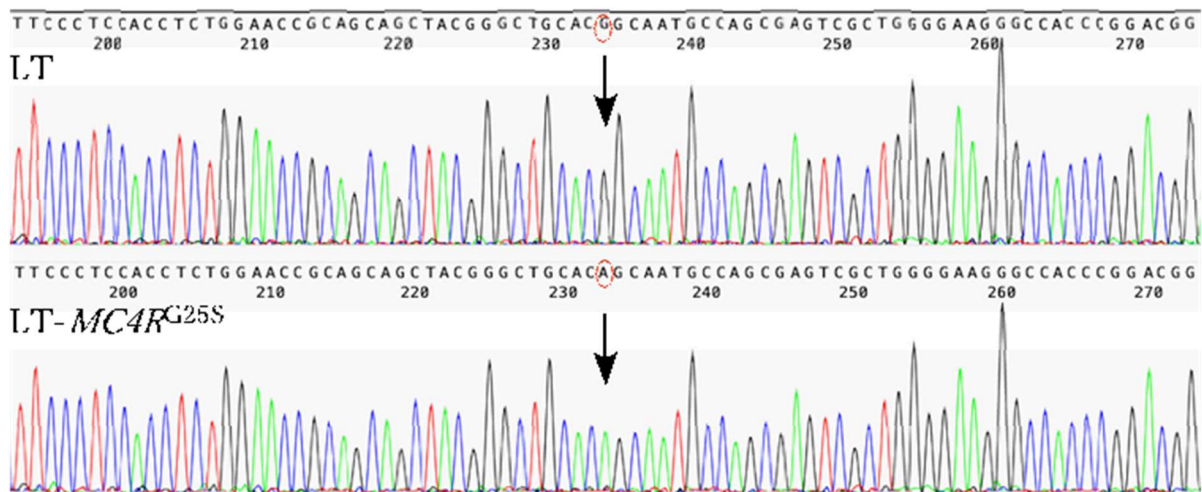


Figure 5. *MC4R* gene editing in the LT strain.

(A) Design of gRNAs to induce single-nucleotide exchange in *MC4R* cells. Sequences of gRNAs within the target sequence for genome editing are indicated by underlines. The sequence of a single-stranded oligodeoxynucleotide (ssODN) corresponding to the 129 strain is indicated below. The target nucleotides exchanged are indicated in red.

(B) The results of DNA sequencing analysis of LT and LT-*MC4R*^{G25S} strains are indicated. The target nucleotides exchanged are indicated by red circles.

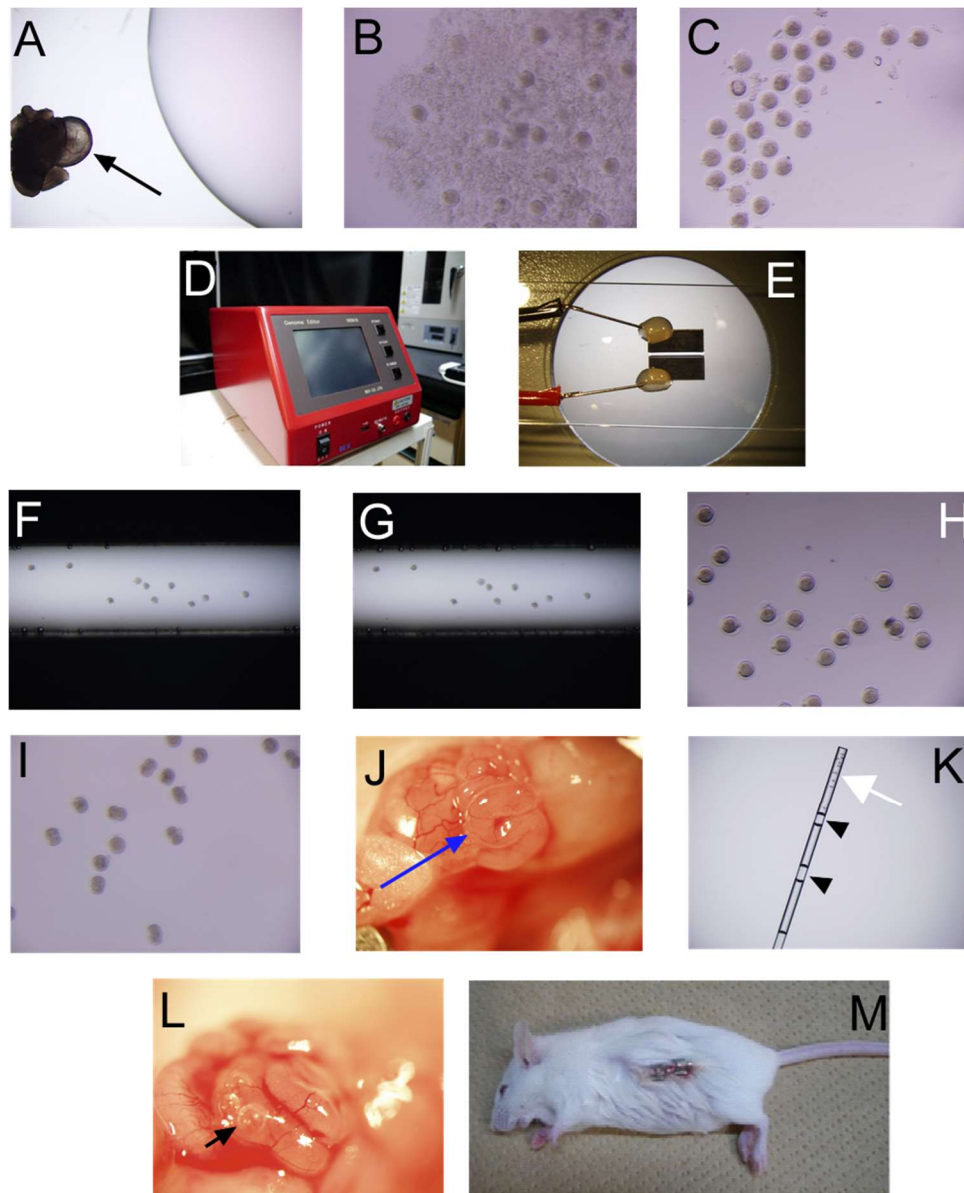


Figure 6: Pathways for gene edited mouse creation.

1st step: Fertilized egg collection (A) Fallopian tubes before egg collection; ampulla (Black arrow) of uterine tube (clogged egg). (B) After egg collection. Eggs were covered with cumulus cells. (C) After hyaluronidase treatment cumulus cells were removed, and eggs were separated one by one.

2nd step: Electroporation (D) The electroporator (BEX GEB15) used. (E) Electrodes (LF501PT1-10). (F) State before electroporation. The electrodes contain eggs and reagents (gRNA, CRISP protein, ssODN). (G) State after electroporation. Bubbles adhere to the electrodes. (H) After electroporation culturing for 3 hours. Male and female pronuclei can be observed.

3rd step: Transplantation of 2-cell stage embryos. (I) Embryo on the day of transplantation. Two-cell stage embryos and one-cell embryos are mixed. (J) Fallopian tubes before transplantation. Blue arrow showing the ampulla where fertilized eggs will be transplant. (K) Embryos into the glass capillary (white arrow); air layer inside capillary (black arrowhead). (L) Fallopian tubes after transplantation. Air bubbles in the fallopian tube ampulla (small black arrow) confirmed that the embryo has entered the oviduct. (M) Post surgery state of the host female mouse.

A.

Nucleotides		gRNA1	gRNA2
LT	ATGAACTCCACCCACCACCATGGCATGTATACTTCCCTCCACCTCTGGAACCGCAGCAGCTACGGGCTGCACGGCAATGCCAGCGG-AGTCGCTGGGGAAGGGCCACCCGGACGGAGGAT		
G25SA.....		
-1GA.....		
+2G.....		
-26		
+27		

Amino acids			
LT	MNSTHHHGMYSLSLHLWNRSSYGLHGNASESLGKGHPDGGCYEQLFVSPEVFVTLGVISLLENILVI	332	
G25SS.....	332	
-1-DRWGRATRTE DAMSNFFPPRCL	51	
+2SRWGRATRTE DAMSNFFPPRCL	52	
-26RVAEPRRML	32	
-27-----	323	

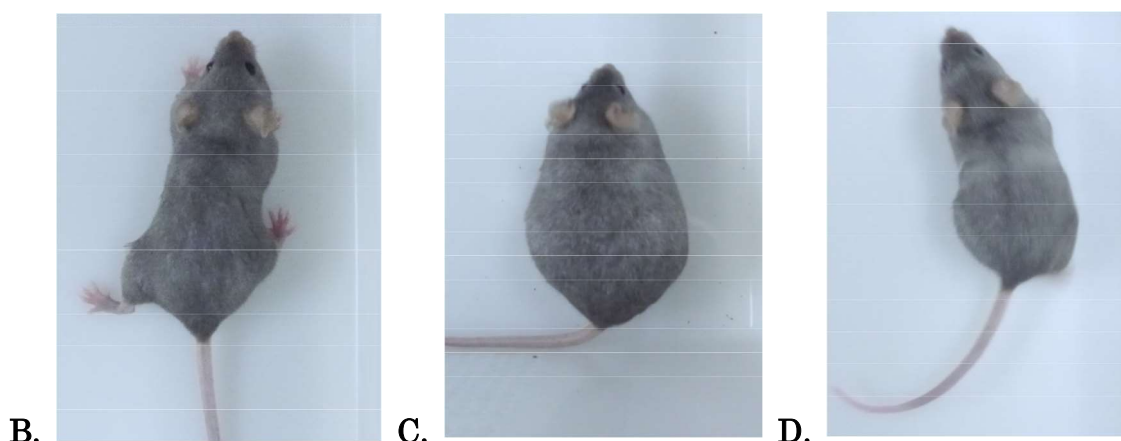


Figure 7: Genotype details of progeny from *MC4R* genome editing.

(A) The positions of sites for gRNAs are indicated by lines. Nucleotide alignment shows deletions (dashes) and insertions at the target site in the strains of mutants. The number of deleted or inserted bases are indicated. Amino acid alignment shows truncated peptides caused by frame shift mutations or deletions. The number of lengths of amino acids of *MC4R* proteins produced in strains are indicated.

(B) The wild type LT mouse. (C) Obese phenotype from *MC4R* knockout mouse (+2bp insertion) proving success of genome editing. (D) Knock-in *MC4R*^{G25S} mouse.

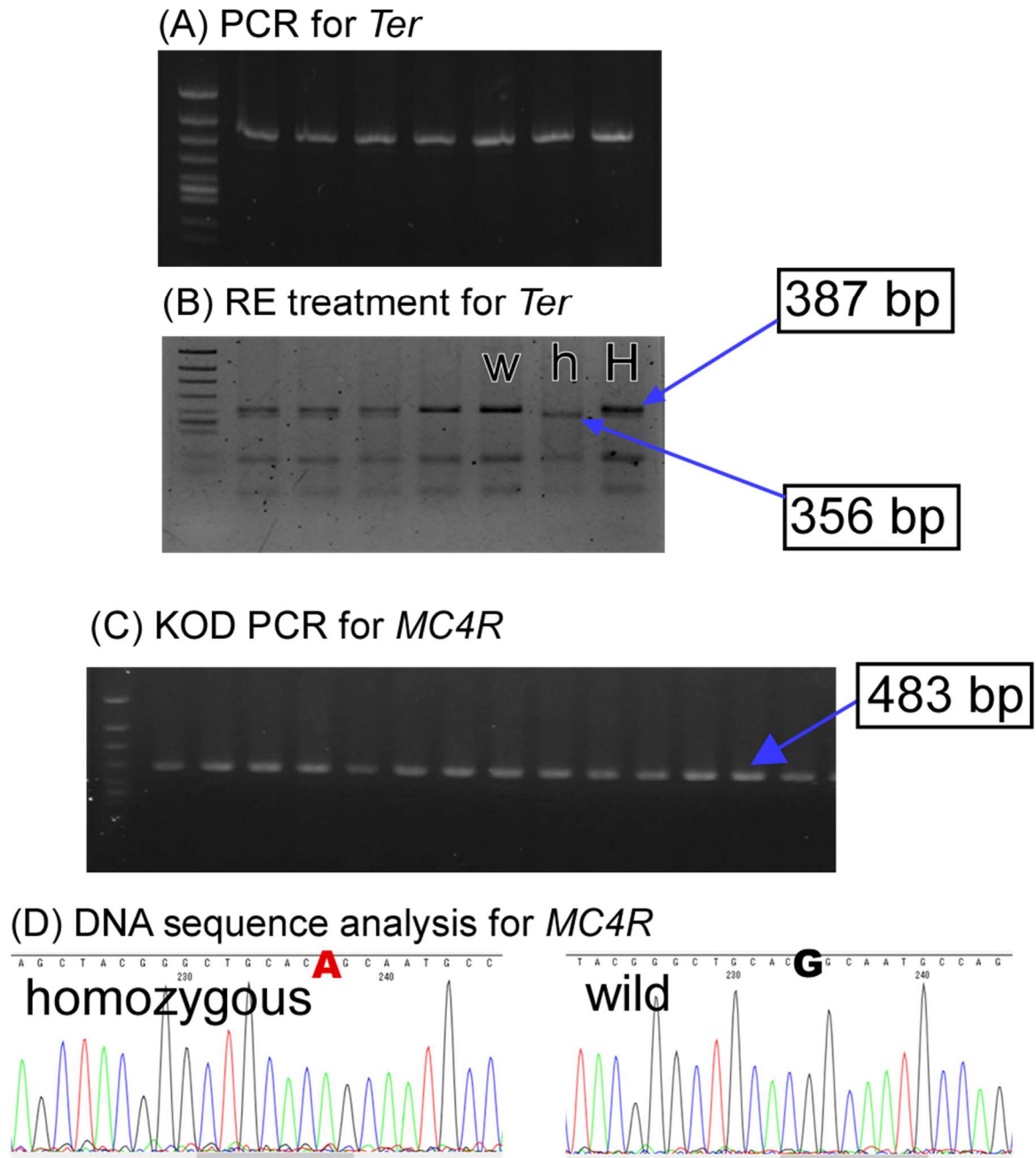


Figure 8: Mouse genotyping techniques for *Ter* & *MC4R* genes.

Genotyping for *Ter*: PCR-RFLP method used to check genotype for *Ter* gene. (A) PCR (B) RFLP by restriction enzyme treatment test. Wild and homozygous individuals are confirmed by their band size 387 bp and 356 bp respectively.

Genotyping for *MC4R*: To identify genotype of *MC4R* gene DNA sequencing method was needed as no specific restriction enzyme was identified for PCR-RFLP. (C) KOD PCR, (D) DNA sequencing. In case of knock-in G is replaced by A.

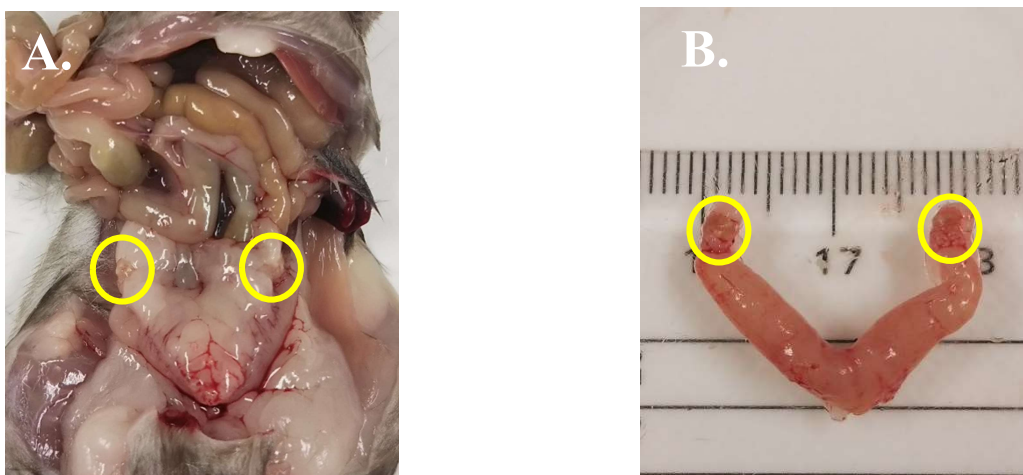


Figure 9 (i): A LTXBJ ♀ (90 days old) with normal reproductive system.

A. After dissection B. Left & right ovaries (3mm in dm & 0.2g in weight in avg.)
 [Scale bar = In cm]

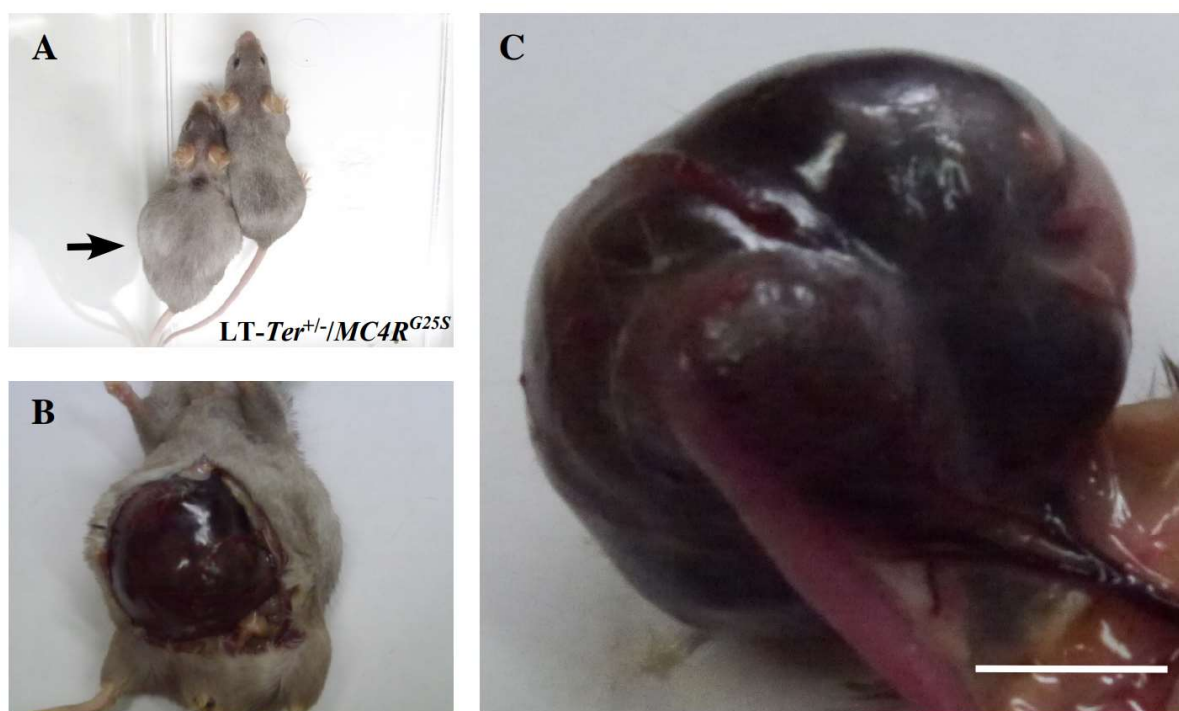


Figure 9 (ii): Teratoma formation in the double genetically modified strain $LT-Ter^{+/-}/MC4R^{G25S/G25S}$.

(A) A photograph of females of the $LT-Ter^{+/-}/MC4R^{G25S}$ strain. The mouse on the left side had a swollen abdomen than a normal female on right. (B) A developed ovarian teratoma was found in the swollen abdomen upon dissection. (C) An enlarged image of the ovarian teratoma from B.
 [Scale bar = 1 cm]

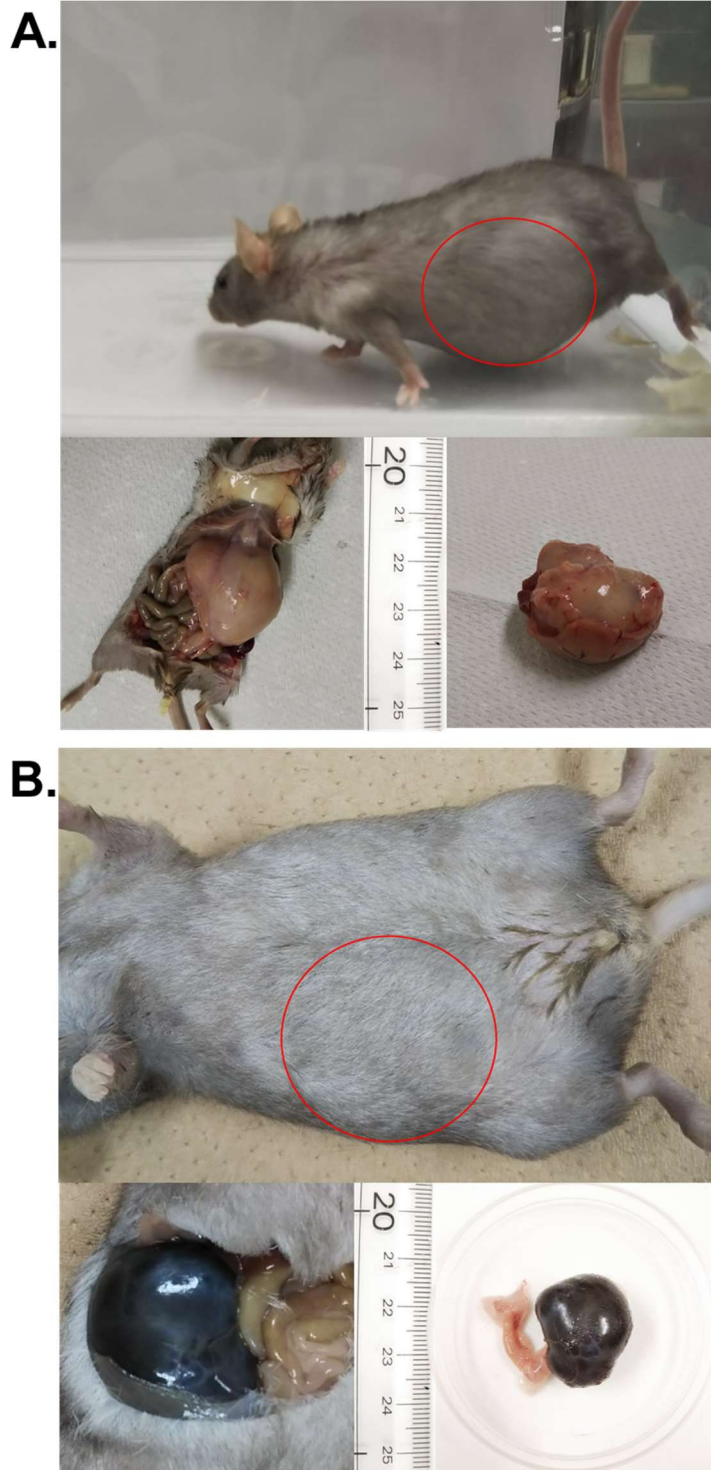


Figure 10: Morphologies of teratomas found in two specimens of *LT-Ter^{-/-}/MC4R^{G25S/G25S}* strains.

(A) The first case is from F2 generation (F2-5 28b) where the abdomen heavily enlarged as pregnant female mouse (red circle in upper panel); after dissection (lower panel) the teratoma excised from the body which fused with peritoneal layer and difficult to distinguish the ovary. (B) The second case is from F5 generation (F5-20 59a). Here blackish, enlarged right ovary form teratoma while the left ovary is in normal shape and structure. [Scale = In cm]

A. $LT-MC4R^{G25S}$ **B.** $LT-Ter^{+/+}/MC4R^{G25S}$ **C.** $LT-Ter^{+/-}/MC4R^{G25S}$

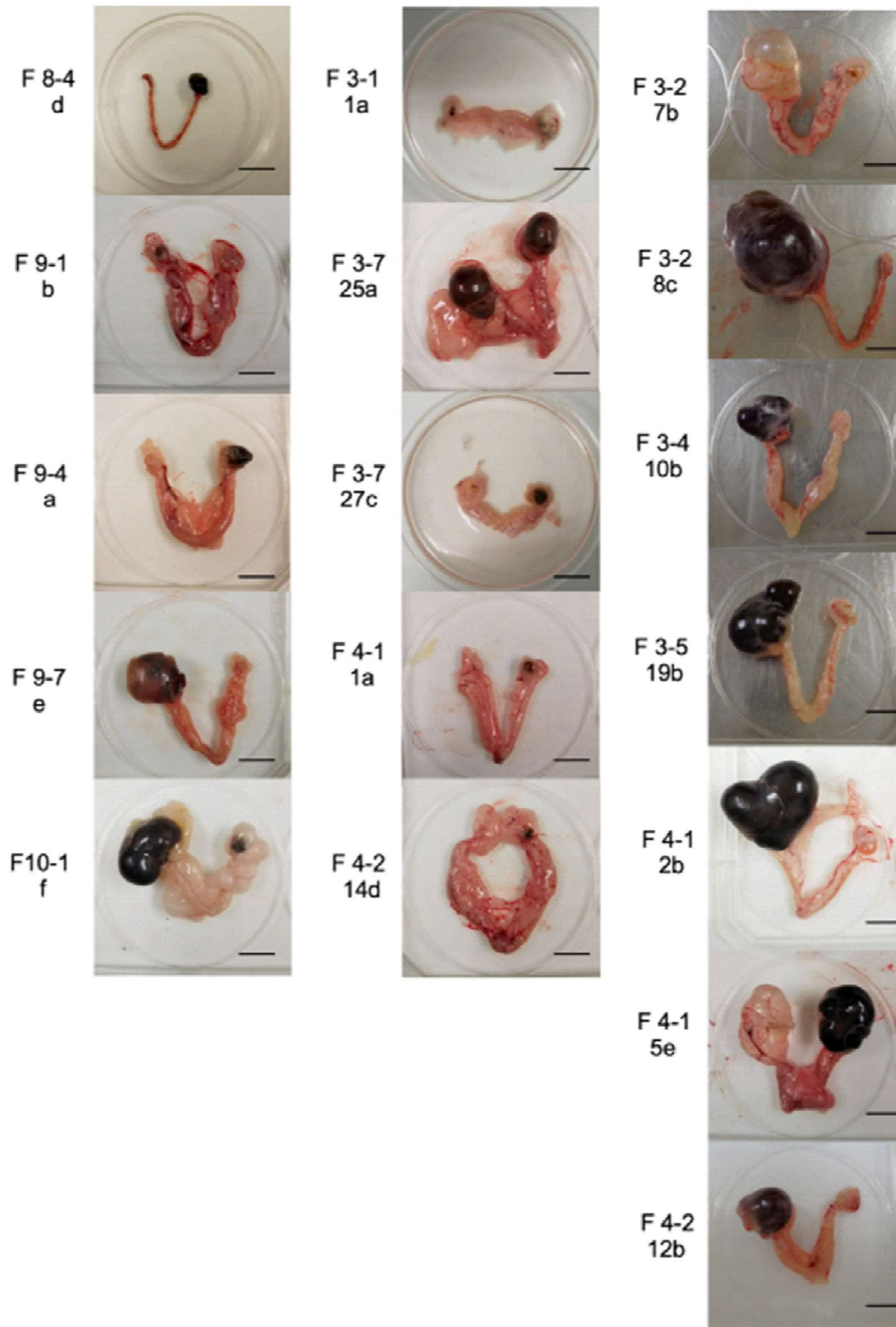


Figure 11: Morphologies of teratomas found in $LT-MC4R^{G25S}/G25S$, $LT-Ter^{+/+}/MC4R^{G25S}/G25S$ and $LT-Ter^{+/-}/MC4R^{G25S}/G25S$ strains.

Females older than three months old or older were dissected and ovaries were excised and photographed. (A) Five specimens from $LT-MC4R^{G25S}/G25S$, (B) Ten specimens from $LT-Ter^{+/-}/MC4R^{G25S}/G25S$ and (C) One specimen from $LT-Ter^{+/-}/MC4R^{G25S}/G25S$. Scale bar = 1 cm

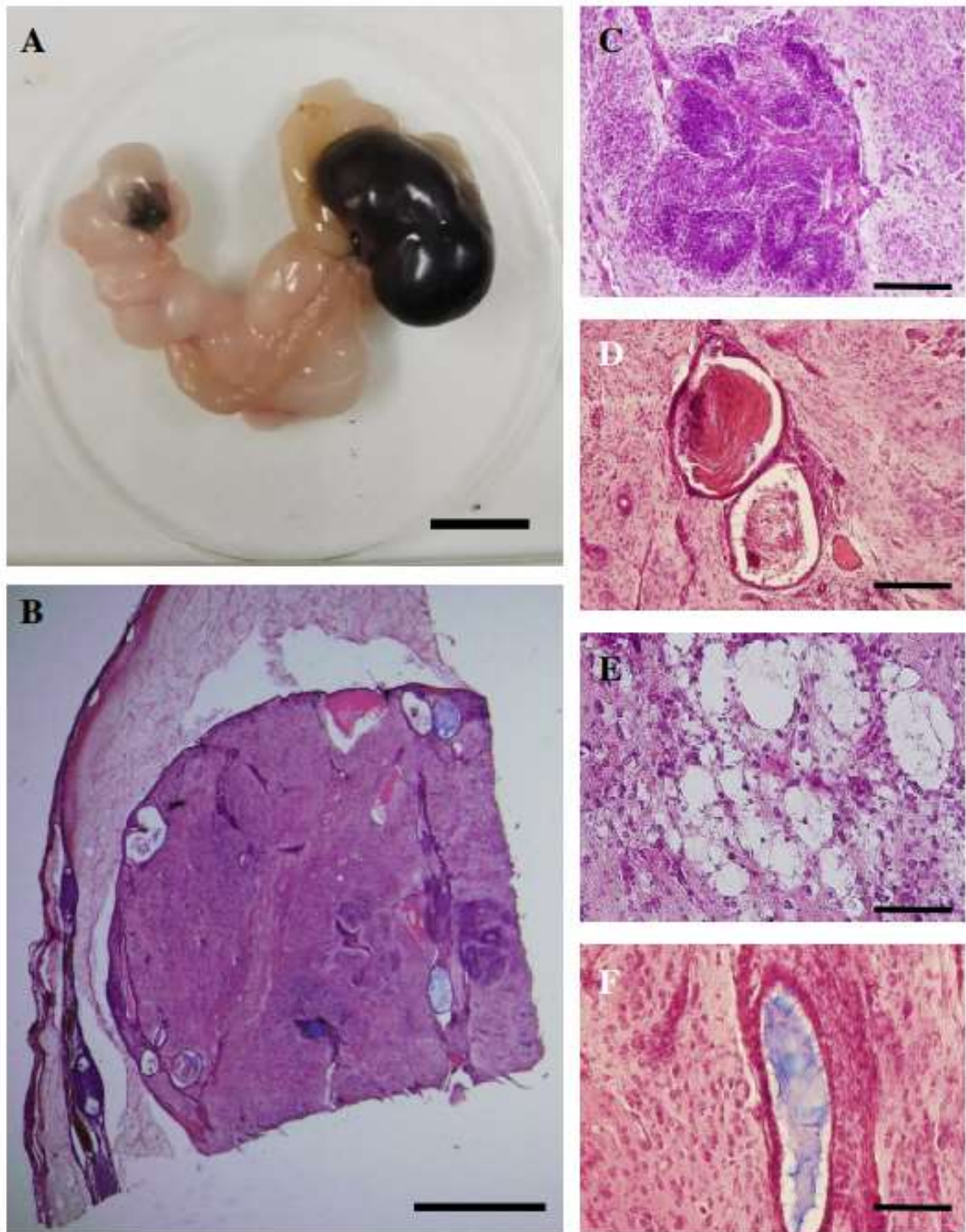


Figure 12: Teratoma formation in the knock-in strain *LT-MC4R^{G25S}*.

(A) An ovarian teratoma found in a female of the *LT-MC4R^{G25S}* strain. (B) A representative histological section of a developed ovarian teratoma. Scale bar = 100 μm . (C-E) Photographs of tissue-like structures found in a teratoma: C, neuronal tissue; D, keratin pearl; E, adipose tissue; F, mucinous glandular structure with ciliated epithelium. Scale bars = 200 μm .

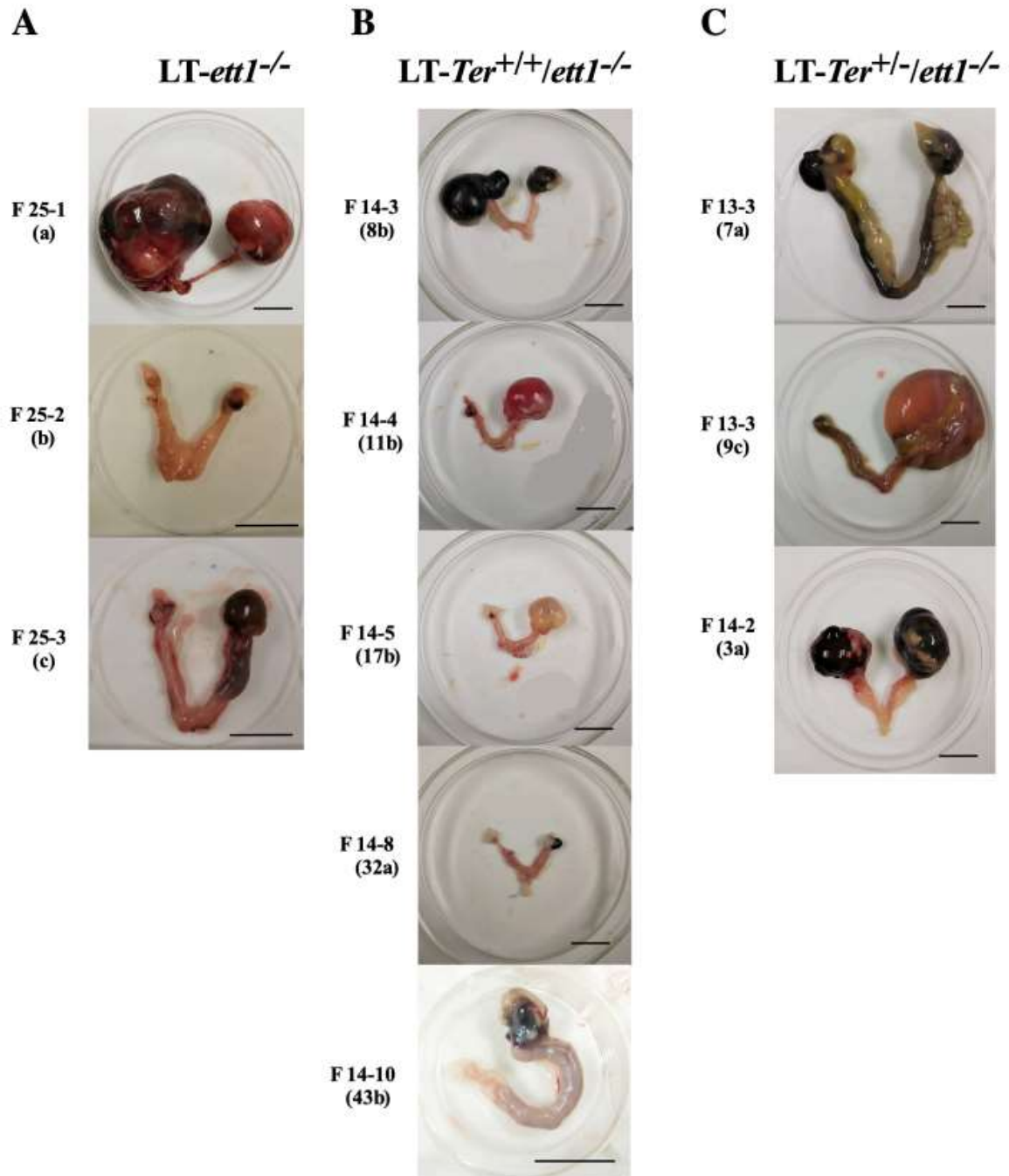


Figure 13: Morphologies of teratomas in *LT-ett1^{-/-}*, *LT-Ter^{+/+}/ett1^{-/-}* & *LT-Ter^{+/-}/ett1^{-/-}* strains.

Females older than three months old or older were dissected and ovaries were excised and photographed. (A) Three specimens from *LT-ett1^{-/-}*, (B) Five specimens from *LT-Ter^{+/+}/ett1^{-/-}* and (C) Three specimen from *LT-Ter^{+/-}/ett1^{-/-}*. Scale bar = 1cm.

/	=	no change LTXBJ
+/+	=	wild for <i>Ter</i>
+/-	=	heterozygous for <i>Ter</i>
-/-	=	homozygous for <i>Ter</i>
H	=	heterozygous for <i>ett1</i> & <i>MC4R</i> ^{G25S}
h	=	homozygous for <i>ett1</i> & <i>MC4R</i> ^{G25S}

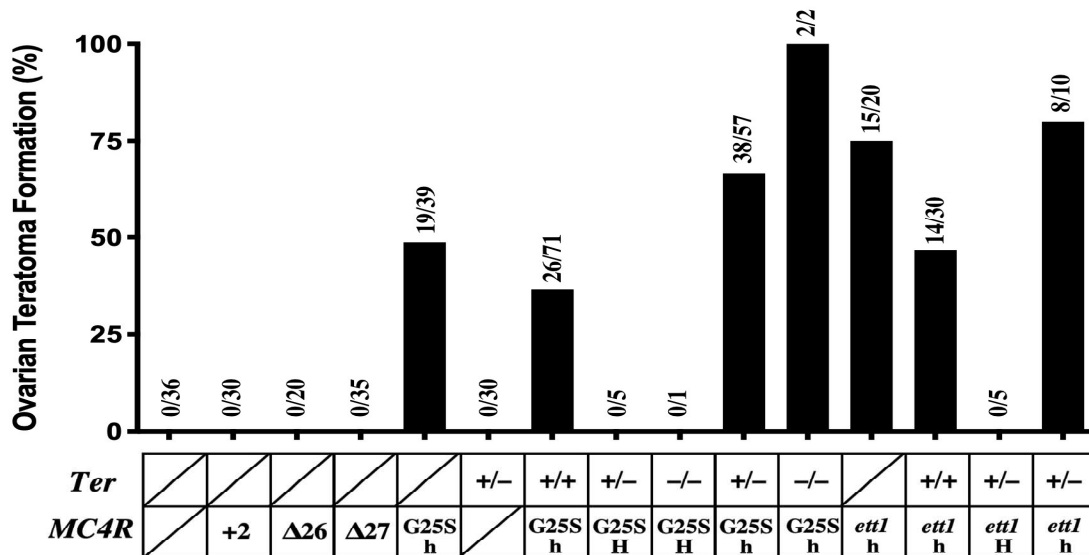
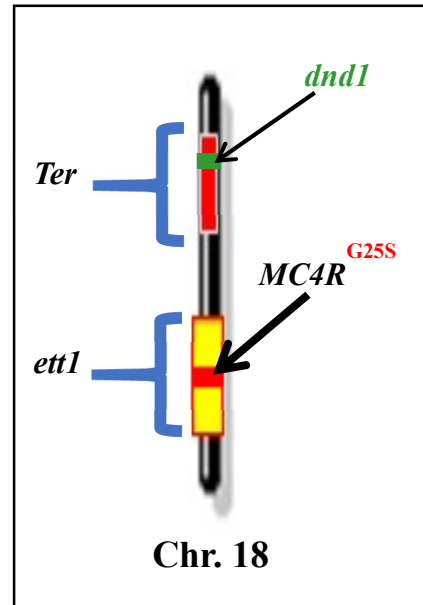


Figure 14: Incidence of ovarian teratoma formation in various strains.

The genetic background of all the strains is LT. Numbers on columns represent numbers of teratoma-developing mice among the total numbers of mice checked. The table under the bars represents the genotypes of each strain. A slash in a square indicates no genetic change from LT. Upper row indicates the exchange of the *Ter* region between strain 129. Lower row indicates changes in the *ett1* region (insertion, deletion or knock-in in the *MC4R* gene or the exchange of the *ett1* region). [Upper right panel showing a schematic diagram for Chromosome 18 of mouse indicating the position of *Ter* & *ett1* loci and *dnd1* & *MC4R*^{G25S} genes respectively]

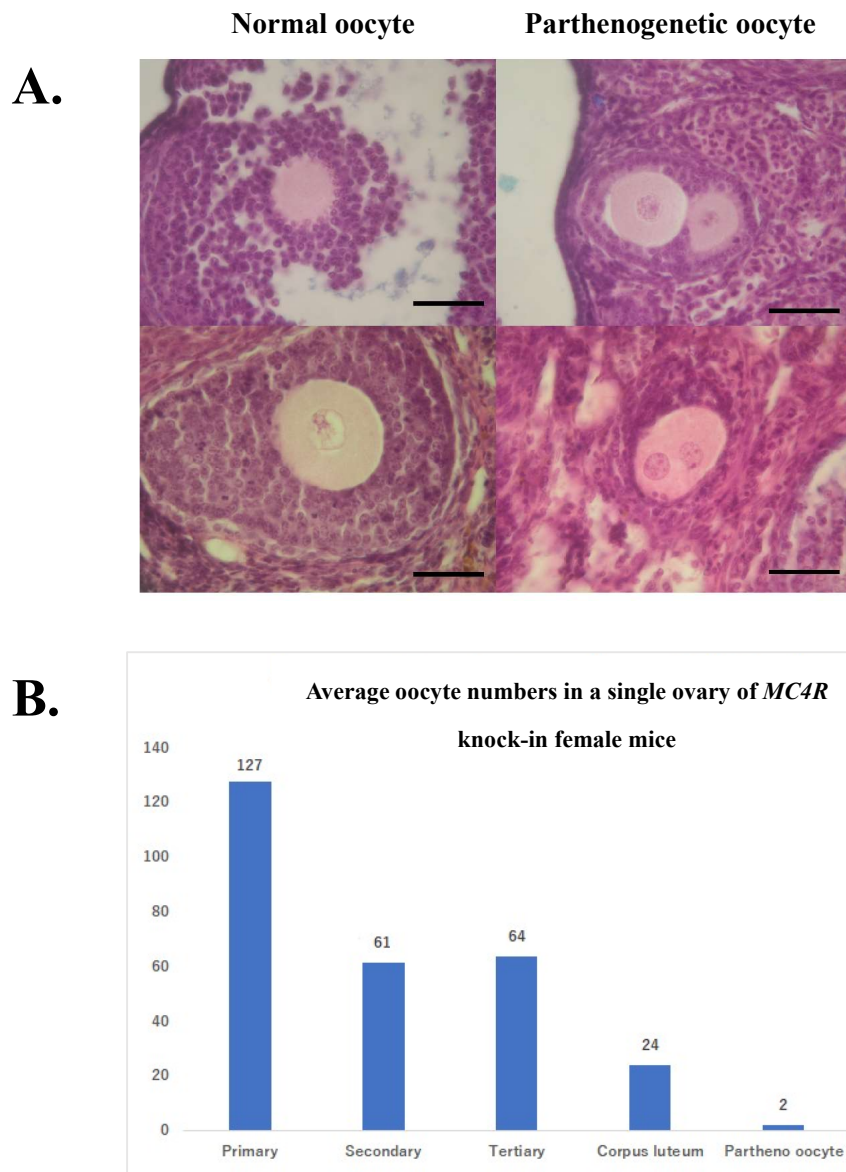


Figure 15: Parthenogenesis of oocytes in the *MC4R* knock-in strain.

- A. Representative sections of ovaries from one-month-old females of the LT-*MC4R*^{G25S} strain. Normal oocytes in developed follicles are indicated on the left side. Two cell stage blastomeres in small follicles are shown on the right side. [Scale bars = 100 μ m]
- B. Graph showing the average numbers of oocytes, corpus luteum and parthenogenetic oocytes in a single ovary from *MC4R*^{G25S} knock in female mice.

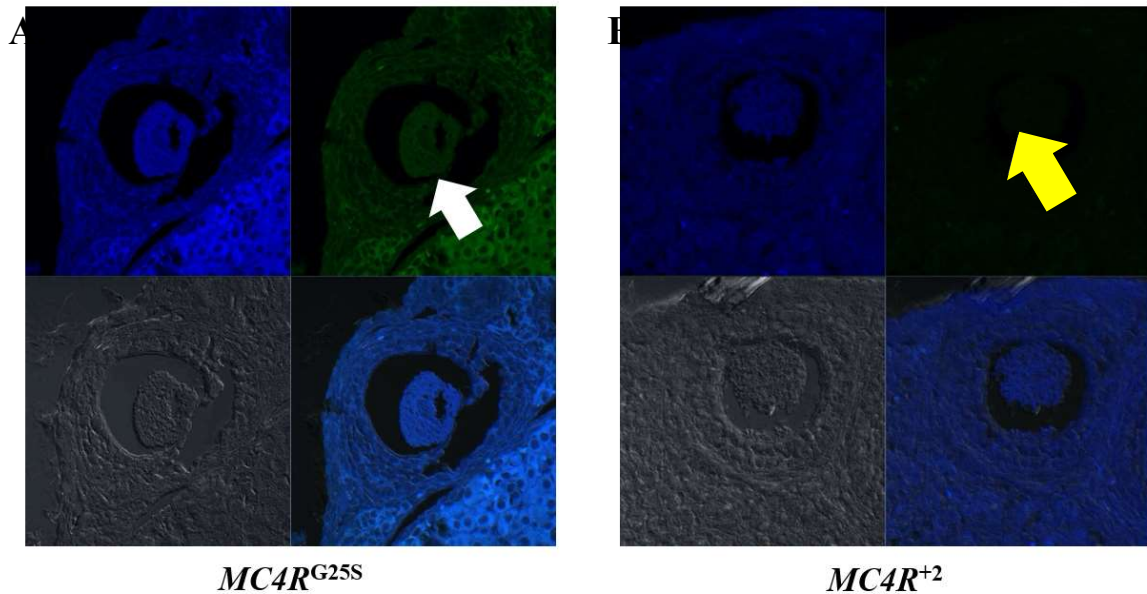
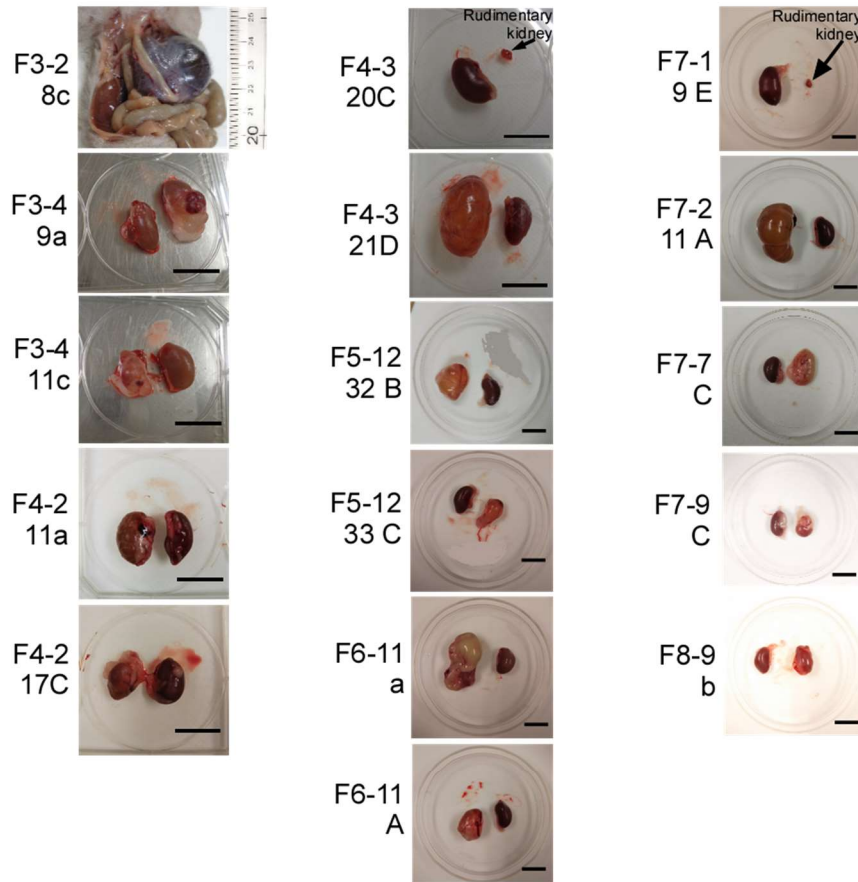


Figure 16: *MC4R* expression in oocytes.

- A.** Immunohistochemical staining results of sections of ovaries from one-month-old females of the knock-in LT- $MC4R^{G25S}$ strain. Sections were stained with anti- $MC4R$ antibody. Oocyte is indicated by **white** arrowhead. Scale bars = 200 μ m.
- B.** Immunohistochemical staining results of sections of ovaries from one-month-old females of the knockout LT- $MC4R^{+2}$ strain. As a negative control $MC4R$ blocking peptide was used to react with primary antibody. Position of oocyte is indicated by **yellow** arrowhead. Scale bars = 200 μ m.

A. $LT-Ter^{+/-}/MC4R^{G25S/G25S}$



B. $LT-Ter^{+/+}/MC4R^{G25S/G25S}$

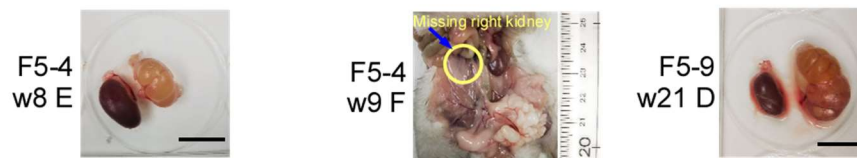


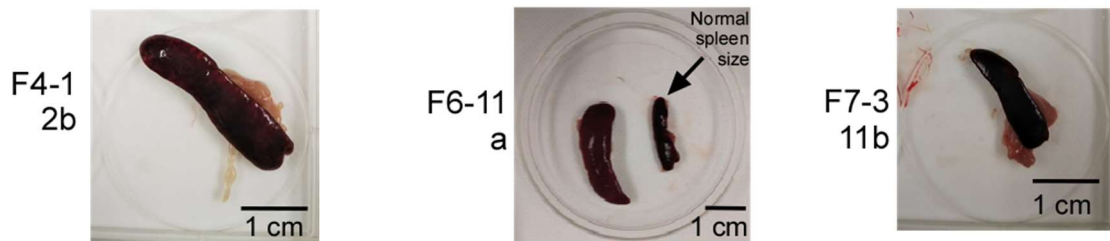
Figure 17: Morphologies of kidney abnormalities found in $LT-Ter^{+/-}/MC4R^{G25S/G25S}$ and $LT-Ter^{+/+}/MC4R^{G25S/G25S}$ mice strains.

During OTs observation abnormal kidney first observed in F 3-2 8c female. Usually kidney getting robust fluid filled red, brown, or yellow color. Two cases have been observed with rudimentary or lack of one kidney. (A) 16 specimens from $LT-Ter^{+/-}/MC4R^{G25S/G25S}$ and (B) 3 specimens from $LT-Ter^{+/+}/MC4R^{G25S/G25S}$. [Scale bar = 1 cm]

A. $LT-Ter^{-}/MC4R^{G25S/G25S}$



B. $LT-Ter^{+}/MC4R^{G25S/G25S}$



C. $LT-MC4R^{G25S/G25S}$

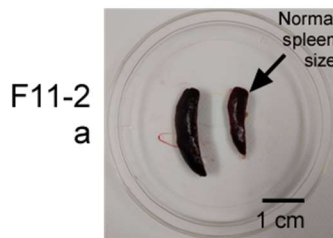


Figure 18: Morphologies of spleen abnormalities found in, $LT-Ter^{-}/MC4R^{G25S/G25S}$, $LT-Ter^{+}/MC4R^{G25S/G25S}$ and $LT-MC4R^{G25S/G25S}$ mice strains.

During OTs observation abnormal spleen was first observed in double homozygous female mutant mouse F 2-5 28b. Usually spleen getting robust, elongated, and blackish in color. (A) Two specimens from $LT-Ter^{-}/MC4R^{G25S/G25S}$ (B) 3 specimens from $LT-Ter^{+}/MC4R^{G25S/G25S}$ (C) One specimen from $LT-MC4R^{G25S/G25S}$. [Scale bar = 1cm]

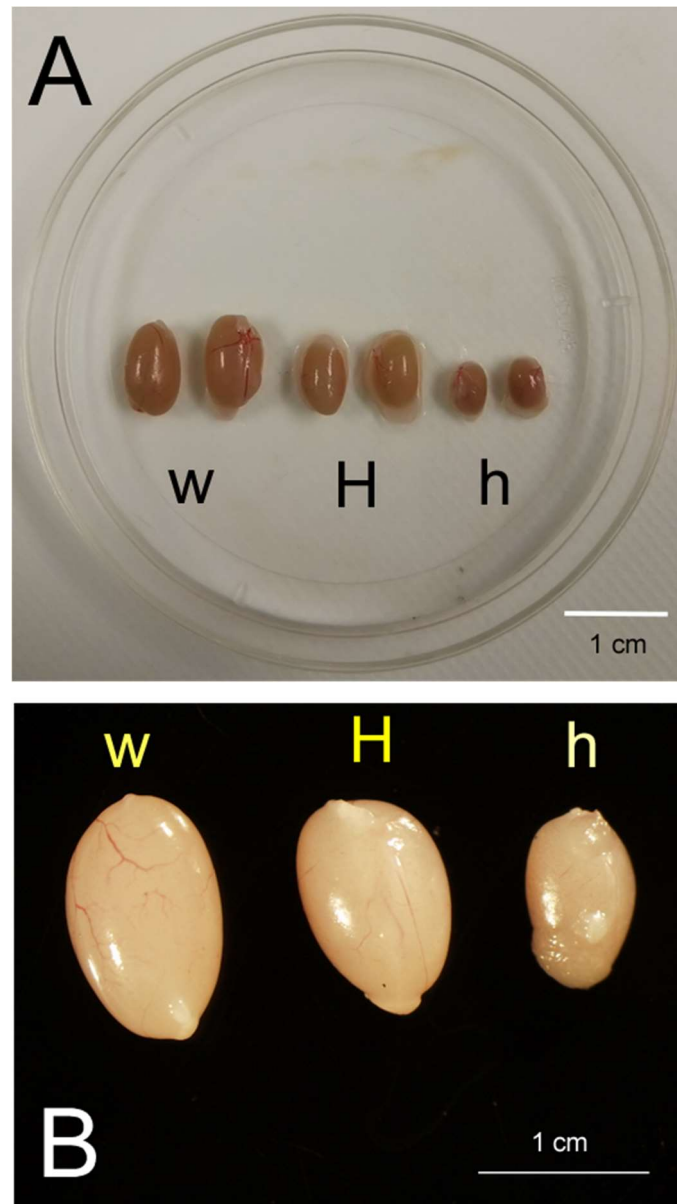


Figure 19: Morphologies of testis comparing wild, heterozygous, and homozygous type in *Ter* mutation of *LT-Ter/MC4R^{G25S}* and 129/Sv mice strains.

(A) Testis of *LT-Ter/MC4R^{G25S}* double mutant mouse strain, (B) Testis of 129/Sv mice strains. There are no STT or morphological abnormalities have been observed in the testis of *LT-Ter/MC4R^{G25S}* males except the reduced in size in heterozygous and homozygous *Ter* conditions.

Appendices

Appendix Table 1: *Ter* loci genotyping in the LT-*Ter/ett1* double congenic strain. The results of the SSLP analysis using microsatellite markers are summarized.

Marker	cM	Start (Mbp)	<i>Ter</i> ^{+/+}	<i>Ter</i> ^{+/-}	<i>Ter</i> ^{-/-}
D18Mit64	4.46	6.1	LT	LT	LT
D18Mit84	18.21	33.8	129	129	129
<i>Dnd1</i> ^{Ter}	19.46	36.8	LT	H	129
D18Mit17	21.09	39.5	LT	H	129
D18Mit163	23.29	43.4	LT	H	129
D18Mit235	23.80	44.7	LT	H	129
D18Mit58	24.56	46.4	LT	H	129
D18Mit24	27.12	50.0	LT	LT	LT
D18Mit55	28.92	53.2	LT	LT	LT
D18Mit123	30.12	56.0	LT	LT	LT
D18Mit152	34.78	61.9	129	129	129
D18Mit40	37.11	63.7	129	129	129
D18Mit81	39.53	66.5	129	129	129
D18Mit184	39.70	66.8	129	129	129
D18Mit9	42.56	68.5	129	129	129
D18Mit33	43.49	69.7	129	129	129
D18Mit103	44.19	70.2	129	129	129
D18Mit186	45.63	72.0	LT	LT	LT
D18Mit49	51.27	76.0	LT	LT	LT
D18Mit47	52.38	77.8	LT	LT	LT
D18Mit126	52.67	78.9	LT	LT	LT
D18Mit4	57.53	84.1	LT	LT	LT

Appendix Table 2: Result summary and status of genome edited mice strains.

Strain	genome	aa	phenotype	Current generation & Pairing type (Genotype)
LT- <i>Mc4r</i> ⁺²	4 bp substitution & 2 bp insertion	Early stop codon with frameshift (V 52 X)	Obesity	F8 In cross (Homozygous)
LT- <i>Mc4r</i> ^{A26}	26 bp deletion	Early stop codon with frameshift (G 31 X)	Obesity	Strain abolished (same phenotype as LT- <i>Mc4r</i> ⁺²)
LT- <i>Mc4r</i> ^{A27}	27 bp deletion	Deficiency of 9 amino acid residues (20-28)	-	F9 In cross (Homozygous)
LT- <i>Mc4r</i> ^{G25S}	G73A	G 25 S	-	F13 In cross (Homozygous)
LT- <i>Mc4r</i> ^{A1}	1 bp deletion	Early stop codon with frameshift (T 53 X)	Sterile	Stopped
LT- <i>Mc4r</i> ^M	Mosaic mutation	?	?	Not continued (because of unknown genotype)

Acknowledgements

I sincerely express gratitude to honourable Professor Toshinobu Tokumoto (PhD), Dept. of Bio-science, GSST, Shizuoka University; my academic supervisor who cooperated in every aspects of my life after I came to Japan. He always inspired, helped, taught with care and gently to make me clear on each and everything related to not only molecular biology but other field also. I always found him patient as he spread his knowledges to me and other students. I never meet such an honourable research personnel to conduct research broadly into various field at a time. It was him to make me more patient whenever I stuck during my research and give me hope which finally become fruitful to access my research findings.

I felt my warmest thanks to my co-supervisors and all teachers of my departments for their support and help during my study. I am also incredibly grateful to the GSST, Shizuoka University for giving me such opportunity to conduct my research. Additionally, thankful to ABP (Asia Bridge Program) committee for creating great opportunities for me, as well as other foreign students to complete MS degree which help me to enrolled in PhD research arena in Shizuoka University.

I also indebtedly thankful to my former lab-mate and senior sister Mst. Afroza Akhter who introduced me to Tokumoto sensei and created an opportunity for doing research in my childhood dream country, Japan and nice compassionate, advices during her staying.

I am grateful to my co-authors who played important part during this study. Especially, I want to say thanks to Miyazaki San, who beginning this study by creating

genome edited mice which I have been used during my study.

I also convey my special thanks to Dr. Md. Nurul Islam, my previous supervisor from University of Rajshahi, Bangladesh for his endless effort to lead me into research arena during my undergraduate period until I came abroad.

I would like to express my heartiest gratitude to my parents who always inspire me towards education from my childhood and without their prayer & love it was impossible for me to be here.

Finally, none other than my adored wife, Anamika Paul and son Anaam Anno who also cross over challenging hurdles throughout this foreign life by enormously giving me support both mentally, morally which made me more focus to carry out research and study.

The Author

Thesis	The <i>MC4R</i> gene is responsible for the development of ovarian teratomas (<i>MC4R</i> 遺伝子は卵巣性テラトーマ発症の原因遺伝子である) Abdullah An Naser	December 2020
--------	---	------------------